Heli Kangas

Surface chemical and morphological properties of mechanical pulps, fibers and fines

KCL
re-inventing paper

Surface chemical and morphological properties of mechanical pulps, fibers and fines

Heli Kangas

ABSTRACT

The aim of this work was to study the surface chemical and morphological properties of different mechanical pulps with special focus on the effects of refining, bleaching and enzymatic modification on the surface properties of the isolated pulp fractions, namely fibers, fibrillar fines and flake-like fines. Special emphasis was placed on evaluating the suitability of time-of-flight secondary ion mass spectroscopy (ToF-SIMS) for studying the surface chemical properties of pulps and pulp fractions. Electron spectroscopy for chemical analysis/x-ray photoelectron spectroscopy (ESCA/XPS) was used to complement and/or verify the results given by ToF-SIMS. The morphological properties of pulps and pulp fractions were studied by atomic force microscopy (AFM) and field emission scanning electron microscopy (FE-SEM).

ToF-SIMS proved to be a valuable tool for studying the surface chemistry of mechanical pulps. For example, the content of guaiacyl units in the surface lignin could be determined and used to indicate which cell wall layer was exposed. The higher the intensity of peaks originating from guaiacyl lignin units, the higher the proportion of inner cell wall layers. ToF-SIMS can also identify several types of surface extractives based on their molecular masses and characteristic peaks in the spectra. However, ToF-SIMS cannot be considered to be a quantitative method for organics, and ESCA/XPS is therefore needed to complement the results.

The surface chemical and morphological properties of fibers differed from those of fines. The surfaces of fines contained more extractives and lignin, while the surfaces of fibers were richer in polysaccharides. Different types of fines also exhibited different surface properties, fibrils having more extractives on their surface and flakes more granular lignin. Refiner and groundwood pulps and pulp fractions differed in their surface chemical properties due to differences in the pulping processes.

Increased refining energy raised the intensity of peaks originating from guaiacyl lignin units on the surface of fibers, which together with FE-SEM images reflected the increased exposure of the secondary wall layer. The surface chemical properties of fines showed that at low specific energy consumption fibrils were formed from the outer fiber wall layers (P+S1), but the content of secondary wall material increased as a function of refining energy. At the start of refining, flakes originated from compound middle lamella (ML+P) but during later refining stages they were also released from the outer secondary wall (S1).

ToF-SIMS also indicated a decrease in the surface content of chromophores of coniferaldehyde origin during mechanical pulp bleaching. Bleaching was found to be effective in removing surface extractives, especially from the surface of fibrils. Lipase and laccase treatments combined with washing selectively removed extractives from the surface of mechanical pulps, especially from the surface of fibrils, and thus increased the hydrophilicity of the pulp.

TIIVISTELMÄ

Työn tarkoituksena oli tutkia mekaanisten massojen pintakemiallisia ja morfologisia ominaisuuksia sekä erityisesti niitä muutoksia, joita massoissa tapahtuu jauhatuksen, valkaisun ja entsymaattisten käsittelyjen aikana. Tavoitteena oli myös tutkia erilaisten mekaanisten massojen pintaominaisuuksien lisäksi massoista eristettyjen fraktioiden, eli kuitujen ja erilaisten hienoaineiden, pintakemiallisia ja –morfologisia ominaisuuksia. Pääpaino työssä oli lentoaikaerotteisen sekundaari-ionimassaspektometrin (time-of-flight secondary ion mass spectrometry, ToF-SIMS) antamilla tuloksilla. Näitä tuloksia tukemaan ja täydentämään käytettiin kemialliseen analyysiin tarkoitettua elektronispektroskopiaa, joka tunnetaan myös nimellä röntgensäde fotoelektronispektroskopia (electron spectroscopy for chemical analysis, ESCA/x-ray photoelectron spectrosopy, XPS). Massojen ja niistä eristettyjen fraktioiden morfologisten ominaisuuksien analysoimiseen käytettiin atomivoimamikroskooppia (atomic force microscopy, AFM) sekä pyyhkäisyelektronimikroskooppia (field emission scanning electron microscope, FE-SEM).

ToF-SIMS soveltui hyvin mekaanisten massojen ja massafraktioiden pintakemiallisten ominaisuuksien tutkimiseen. Laitteella voitiin esimerkiksi analysoida pinnassa olevan ligniinin guajasyyliyksiköiden suhteellinen pitoisuus. Kyseisen tiedon avulla voitiin esimerkiksi arvioida, onko pinnan ligniini peräisin soluseinän uloimmista vai sisemmistä kerroksista. ToF-SIMS:in avulla voitiin myös analysoida pinnassa olevien eri uuteaineryhmien suhteellisia pitoisuuksia. ToF-SIMS ei kuitenkaan ole kvantitatiivinen menetelmä orgaanisille aineille ja niinpä ESCA/XPS:n tuloksia tarvitaan täydentämään ToF-SIMS:in antamia tuloksia.

Mekaanisten massojen kuitujen pintakemialliset ja morfologiset ominaisuudet poikkesivat massojen hienoaineen pintaominaisuuksista. Hienoaineen pinnalla oli enemmän uuteaineita ja ligniiniä kuin kuitujen, ja kuitujen pinnassa oli vastaavasti eniten polysakkarideja. Erityyppisillä hienoaineilla, fibrilleillä ja lastumaisella hienoaineella, oli myös erilaiset pintakemiat. Fibrillien pinnassa oli enemmän uuteaineita ja lastumaisen hienoaineen pinnassa ligniiniä, jotka muodostivat pintaan granuuleja. Hiokkeista ja hierteistä erotetut fraktiot olivat pintakemioiltaan erilaisia.

Jauhatusenergian kasvu lisäsi ligniinin guajasyyliyksiköiden suhteellista pitoisuutta kuitujen pinnalla, joka yhdessä FE-SEM kuvien kanssa kertoi kuituseinämän sisempien kerrosten paljastumisesta. Hienoaineen pintakemiallisia ominaisuuksia analysoimalla voitiin päätellä, että fibrillejä muodostuu jauhatuksen alussa kuituseinämän uloimmista kerroksista (P+S1) ja sekundääriseinästä peräisin olevan fibrillimäisen hienoaineen määrä kasvaa jauhatusenergian kasvaessa. Jauhatusenergian ollessa pieni, lastumaista hienoainesta muodostuu välilamellista sekä primääriseinämästä, mutta jauhatusenergian kasvaessa niitä alkaa muodostua myös uloimmasta sekundääriseinämästä (S1).

ToF-SIMS:in avulla pystyttiin analysoimaan pinnan ligniinin koniferaldehydien suhteellinen pitoisuus, jota voitiin käyttää kromofooristen rakenteiden pitoisuuden indikaattorina. Pinnassa olevien kromofoorien pitoisuus pieneni valkaisun aikana. Valkaisu myös poisti tehokkaasti pinnassa olevia uuteaineita, erityisesti fibrilleistä. Käsittelyjä Lipaasi- ja lakkaasientsyymeillä yhdistettynä pesuun voitaisiin käyttää

uuteaineiden selektiiviseen poistoon massan komponenttien, varsinkin fibrillien, pinnoista, ja siten lisätä massojen hydrofiilisyyttä.

LIST OF PUBLICATIONS

This thesis mainly consists of the results reported in five publications and referred to in the text by their Roman numerals. Some additional unpublished data are also presented.

I Kleen, M., Kangas, H. and Laine, C. (2003). Chemical characterization of mechanical pulp fines and fiber surface layers. Nord. Pulp Paper Res. J. 18(4):361-368.

II Kangas, H. and Kleen, M. (2004). Surface chemical and morphological properties of mechanical pulp fines. Nord. Pulp Paper Res. J. 19(2):191-199.

III Kangas, H., Pöhler, T., Heikkurinen, A. and Kleen, M. (2004). Development of the mechanical pulp fiber surface as a function of refining energy. J. Pulp Paper Sci. 30(11):298-306.

IV Kangas, H. and Kleen, M. (2007). The effect of bleaching on the surface chemistry of mechanical pulps. J. Pulp Paper Sci., accepted.

V Kangas, H., Suurnäkki, A. and Kleen, M. (2007). Modification of the surface chemistry of TMP with enzymes. Nord. Pulp Paper Res. J. 22(4):415-423.

AUTHOR'S CONTRIBUTION

I ToF-SIMS experiments and analysis of the results, manuscript in part

II ToF-SIMS experiments, analysis of all results, manuscript preparation with co-author (responsible author)

III ToF-SIMS experiments, analysis of results excluding the FE-SEM results, manuscript preparation with co-authors (responsible author)

IV ToF-SIMS experiments, analysis of all the results, manuscript preparation with co-author (responsible author)

V ToF-SIMS experiments, analysis of all the results, manuscript preparation with co-authors (responsible author)

PREFACE

LIST OF SYMBOLS AND ABBREVIATIONS

C1, C2, C3,C4	carbon peaks originating from none (C-C), one (C-O), two (O-C-O) and three (O-C=O) bonds to oxygen, respectively
C1s	carbon spectrum from wide spectrum
E_b	binding energy of electron
E_k	kinetic energy of photoelectron
F	force on the tip
G	guaiacyl lignin unit
hv	energy of the X-ray
k	spring constant
m	mass of secondary ion
ML	middle lamella
ML+P	compound middle lamella
L	length of flight path of secondary ion
O1s	oxygen spectrum from wide spectrum
P	primary wall of wood fiber
S	syringyl lignin unit
S1	outer secondary wall of wood fiber
S2	inner secondary wall of wood fiber
t	flight time of secondary ion
z	charge of ion
Z	displacement of the cantilever
V	acceleration voltage
AFM	atomic force microscope
AG	anionic group
AKD	alkenyl ketyl dimer
ASA	alkenyl succinic acid
ATR-IR	attenuated total reflection infrared
Au-Pd	gold-palladium
BE	backscattered electron
BMcNett	BauerMcNett
CFA	coniferaldehyde
CTMP	chemi-thermomechanical pulp
CTMP-P	peroxide bleached chemi-thermomechanical pulp
CSF	Canadian standard freeness
DCM	dichloromethane
DDJ	dynamic drainage jar
DHP	dehydrogenation polymer
d.w.	dry weight
EDS	energy-dispersive x-ray spectrometry
EPMA	electron-probe micro analysis
ESEM	environmental scanning electron microscope
EFC	elemental chlorine free
ESCA	electron spectroscopy for chemical analysis
FE-SEM	field emission scanning electron microscope

FFA+EFA	free and esterified fatty acids
GW	groundwood pulp
HR-SEM	high resolution scanning electron microscope
ISO	international standard organization
LMIS	liquid metal ion source
LiCl$_2$	lithium chloride
MWL	milled wood lignin
m/z	mass charge ratio
O/C	oxygen carbon ratio
OMe	methoxyl group
OsO4	osmium tetroxide
PDMS	polydimethyl siloxane
PGW	pressure groundwood pulp
PS	polysaccharides
RA	resin acids
RDH	rapid displacement heating
RMP	refiner mechanical pulp
S/G	syringyl guaiacyl ratio
SE	secondary electron
SEC	specific energy consumption
SEM	scanning electron microscope
SIMS	secondary ion mass spectrometry
SMA	styrene-maleic imide
ST+SE	sterols and steryl esters
TG	triglycerides
TMP	thermomechanical pulp
TMP-P	peroxide bleached thermomechanical pulp
TMP-Y	dithionite bleached thermomechanical pulp
ToF-SIMS	time-of-flight secondary ion mass spectrometry
XPS	x-ray photoelectron spectroscopy

CONTENTS

1   INTRODUCTION AND OUTLINE OF THE STUDY

The Oxford English Dictionary defines a surface as "the outside part of something", "any of the sides of an object" or "the top or outside layer of something". Surface thus limits a body and separates it from its surroundings. It is the surface that is encountered first when a body is approached. A surface also has interactions with its surroundings and can therefore have properties that differ from those of the rest of the body. A surface layer may be thin but its properties are very important because they are decisive in the first contact between different bodies.

The aim of this work was to gain fundamental knowledge about the surfaces in mechanical pulps. For evaluation purposes, the surface properties of mechanical pulps were further divided into chemical and physical properties. The surface chemical properties include surface composition and surface charge, whereas roughness and surface porosity, for example, can be considered as being physical surface properties. The study of surface properties is a vast and complex field and involves numerous instruments designed for different purposes. In view of this, this study was limited to those surface chemical and morphological characteristics that were considered of greatest interest for pulp and paper making and that can be studied using a few sophisticated surface-sensitive instruments. The most important (and sensitive) of them all was time-of-flight secondary ion mass spectrometry (ToF-SIMS). This instrument was relatively new in the field of pulp and paper research in 2001, when this work was started, the first publication dating back just ten years.

In addition to mechanical pulp surfaces, the study also embraced the different particles forming the concept "mechanical pulp", i.e. fibers, fiber bundles, shives, parts of the fiber wall, ray cells and different types of fines. Many studies have shown that these particles differ in their properties: size, shape, chemistry, flexibility and bonding. They must surely, therefore, also differ in their surface properties. For the study of their surface properties, the different particles were separated from each other and their surfaces analyzed separately. The most interesting fraction turned out to be fines, which could be separated into still further fractions. Fiber surfaces were also studied.

The first step in the experimental work included in the thesis was to examine whether fines and fibers differ from each other in their surface chemical properties (Paper I). The results of this work prompted the study of the surface properties of different mechanical pulps and their fractions, reported partly in Paper II, and an investigation into how these properties change with increasing refining energy (Paper III). The effect of mechanical pulp bleaching on the surface chemical properties of pulps, fibers and fines was studied in the next stage and is reported in Paper IV. Finally, the possibility of modifying the properties of pulp, fiber and fines surfaces by treating the pulp with specific enzymes was evaluated (Paper V).

The goals of this thesis were to obtain fundamental knowledge about the surface chemical and morphological properties of mechanical pulps, fibers and fines and about how these properties change during refining and bleaching, or how they can be modified with enzymes. The suitability of ToF-SIMS for studying the surface chemical properties of

pulps and pulp fractions was evaluated and the results given by ToF-SIMS were complemented and/or verified with electron spectroscopy for chemical analysis, also called x-ray photoelectron spectroscopy (ESCA/XPS). The surface morphological properties of pulps and pulp fractions were also studied and related to their surface chemical properties.

2   SURFACE PROPERTIES OF MECHANICAL PULPS

During the mechanical pulping of wood raw material, fibers are separated from the wood matrix and a fines fraction is generated. The mechanical pulping process can be divided into two main and partly overlapping stages – fiber separation and fiber development (Karnis 1994). The surface properties of mechanical pulp fibers depend on the fracture point of the fibers, whether fracture takes place in the lignin-rich middle lamella or primary wall or in the secondary wall containing more carbohydrates. The fiber development stage influences the surface properties of fibers, since part of the surface material is removed during this stage.

The fines content in mechanical pulps is generally 10-40%. Fines are defined as particles that pass through a round hole of 76 μm in diameter or a nominally 200 mesh screen. Fines have traditionally been divided into two classes – slime stuff and flour stuff – depending on their physical appearance (Brecht and Klemm 1953). Slime stuff contains swellable fibrillar particles, i.e. fibrils and thin lamellae, while flour stuff consists of flake-like fines, i.e. pieces of fiber, middle lamella and cell wall. Fibrillar fines are ribbon-like, cellulose-rich particles with good bonding ability, whereas flakes consist of many types of particles with different shapes and sizes. Flakes are usually lignin-rich and enhance the light scattering properties of the paper, while fibrils improve strength properties (Luukko et al. 1997). Generally it has been thought that in the manufacture of refiner pulps such as thermomechanical pulp (TMP), flakes are generated during the first stages of refining and thus originate from areas with high lignin contents like the middle lamella or primary wall. Fibrillar fines are generated by peeling of the fiber surface from the outer cell wall layers towards the cellulose-rich secondary wall (Heikkurinen and Hattula 1993, Karnis 1994). The surface properties of fines naturally depend on their origin in the cell wall.

ESCA/XPS has been widely used to study the surface chemical properties of mechanical pulps since the 1970s (Dorris and Gray 1978). ESCA/XPS permits determination of the apparent surface coverage of lignin and extractives on the mechanical pulp surface. The analysis depth of ESCA/XPS for organic materials such as wood pulp is in the range 5-10 nm. The drawback of ESCA/XPS is the need to measure both non-extracted and extracted samples before lignin and extractives coverage can be evaluated. Nevertheless, ESCA/XPS is considered to be a quantitative analysis method.

Dorris and Gray (1978) were the first to publish the results of studies of the surface composition of mechanical pulps. They studied the surfaces of groundwood (GW) pulp, refiner mechanical pulp (RMP) and TMP using ESCA/XPS and found that the surface oxygen content decreased in the order SGW > RMP > TMP, indicating that the proportion of cellulose in the surface decreased in the same order. Thus TMP had the lowest surface coverage of cellulose and the highest of lignin. The authors also found that the surface lignin content did not appear to be much greater than the average bulk lignin content

and that the fibers and fines had similar surface compositions. These findings were later challenged by Koljonen et al. (1997), who found the fines fraction of a pressure groundwood (PGW) pulp (Bauer McNett -200 fraction) to be enriched in lignin and extractives. Westermark (1999) also reported the lignin content on the surface of TMP fibers to be slightly higher than the lignin content in the bulk of the material. Börås and Gatenholm (1999a) studied the surface composition of spruce chemi-thermomechanical pulp (CTMP) and proposed, based on their ESCA analysis, that the pulp had a surface composition of 40% carbohydrates, 28% lignin and 32% extractives. In the spruce CTMP pulp analyzed by Mustranta et al. (2000) the corresponding figures were 45% for carbohydrates, 40% for lignin and 15% for extractives, whereas PGW and TMP had slightly more carbohydrate-rich surfaces, less surface lignin and a similar content of surface extractives to CTMP. In a further study of the CTMP process, Börås and Gatenholm (1999b) found fiber fracture to occur in non-sulfonated regions of the fiber wall and that the plane of rupture changes from the carbohydrate-rich secondary wall towards the lignin-rich middle lamella with increased sulfite charge, thus increasing the content of lignin on the fiber surface. Increasing the pre-heating time resulted in partial removal of lignin and extractives by solubilization.

The surface composition of mechanical pulp fines has been studied to some extent with ESCA/XPS. Luukko et al. (1999) found the surface content of extractives on fines to be about 40 times higher than their bulk content, indicating that extractives are re-precipitated on fines surfaces during different stages of the process. The surface lignin content of fines was slightly higher than the bulk content. The opposite was true for the surface carbohydrate content, which was smaller than the bulk content, but increased slightly with decreasing freeness, indicating that the content of more carbohydrate-rich fibrillar material had increased. Mosbye et al. (2003) also found that the surface coverage of carbohydrates was higher and that of extractives and lignin lower in fines produced at later refining stages. Rundlöf et al. (2000) found that fines from white-water have enrichment of extractives on their surface.

The effect of bleaching on the surface of mechanical pulps has also been studied by ESCA/XPS. Analysis of the surface chemical composition of TMP showed that the surface coverage of extractives decreases during peroxide bleaching, while the lignin coverage remains unaffected (Mustranta et al. 2000, Pere et al. 2001, Koljonen et al. 2003) or decreases (Hannuksela et al. 2003). Dithionite bleaching of PGW also decreased the surface coverage of extractives, whereas the lignin coverage remained the same (Koljonen et al. 2003).

As explained in the introduction, the surface chemistry of mechanical pulps can also be studied with another surface spectroscopic method, namely ToF-SIMS. This provides information about the pulp surface in the form of mass spectra. The information comes from the first molecular layer (1-2 nm), making ToF-SIMS more surface-specific than ESCA/XPS . ToF-SIMS is also very sensitive and can detect compounds present in very low amounts in the surface. This can also be a drawback since ToF-SIMS measurements very often suffer from contamination, for example from polydimethyl siloxane (PDMS) or phthalates. In addition, ToF-SIMS provides only qualitative or sometimes semi-quantitative information. The utilization of ToF-SIMS for the study of mechanical pulp

surfaces so far has been limited. However, some results have been published and these will be summarized in Chapter 3.2.3.

For the study of surface morphological properties of mechanical pulps, atomic force microscopy (AFM) has often been used (Moss and Groom 2002). In AFM, a raster-type motion is used to scan the sample surface. By employing phase imaging in AFM, different surface components such as lignin and cellulose may be identified based on the degree of phase shift. With AFM a lateral resolution of the order of a few ångströms may be achieved and very small details on the surfaces can thus be studied.

Hanley and Gray (Hanley and Gray 1994) were able to image a ribbon of fiber wall from black spruce TMP by means of AFM. Using AFM together with ESCA, Börås and Gatenholm (1999a) were able to propose that lignin was located as irregular patches on the CTMP fiber surface, while extractives existed as globular particles spread over both carbohydrates and lignin. Peltonen et al. (2002) were able to identify the cell wall layer that the sample represented based on the orientation of microfibrils. Lignin on the surface of mechanical pulp fibers can appear as granules or as a uniform layer in the AFM images, as suggested by Koljonen et al. (2003).

The morphology of mechanical pulp fibers has also been studied by means of Scanning Electron Microscopy (SEM), mostly in relation to their development during refining (Mohlin 1977, Lidbrandt and Mohlin 1980, Johnsen,et al. 1995, Braaten 1997, Reme et al. 1998). Börås and Gatenholm (1999b) also used SEM images to visualize the change of plane of fiber rupture from secondary wall to middle lamella with increased sulfite charge. Today, sophisticated microscopes such as high resolution SEM (HR-SEM) can be used to obtain images at high magnifications and small details on the pulp surfaces can thus be studied.

3 TIME-OF-FLIGHT SECONDARY ION MASS SPECTROMETRY (TOF-SIMS

3.1 Principle and technique

In a secondary ion mass spectrometry (SIMS) experiment, the sample surface is bombarded with high-energy primary particles (Vickerman 2001). As a result of this bombardment, secondary particles are emitted or sputtered from the sample surface. The secondary particles can be atoms or molecules, either neutral or ionized. The majority of secondary species are neutral, but ions, positive or negative, are the ones that can be detected and analyzed with a mass spectrometer.

The ToF-SIMS instrument consists of four components: the primary particle source, the mass spectrometer, an ion optical system and a detector (Vickerman 2001). An electron source for charge compensation is also needed. One example of ToF-SIMS instrument design from Physical Electronics is shown in Fig. 1. Monoatomic liquid metal ion sources (LMIS) have long been the most commonly used ion sources in modern ToF spectrometers and the metal cations used include gallium (Ga^+), indium (In^+), cesium

(Cs^+), bismuth (Bi^+) and gold (Au^+). However, polyatomic or cluster ion sources have recently gained popularity due to the commercial availability of compact cluster ion sources. The cluster ions used in SIMS experiments include SF_5^+, Au_2^+ and Bi_2^+, Au_3^+ and Bi_3^+ and C_{60}^+. The benefit of cluster ion bombardment is the greater yields obtained in the analysis of molecular species, which enhances the sensitivity of the technique. Fortunately, yield enhancement is not accompanied by an increase in chemical damage to the surface (Wucher 2006). Aimoto et al. (2006) found that the degree of fragmentation decreased when a primary cluster ion beam was used instead of a monoatomic beam. An intensity enhancement of 100-200 was estimated with Au_3^+ bombardment compared to Ga^+ bombardment on polymer materials. Delcorte et al. (2006) reported a yield increase of two orders of magnitude for organic ions with a C_{60}^+ primary ion source as compared to a Ga^+ ion source when analyzing polymer surfaces.
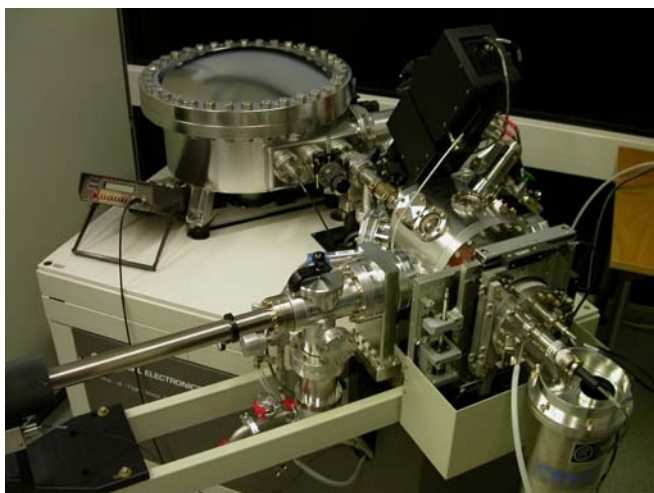
Figure 1. PHI TRIFT II ToF-SIMS, located at Top Analytica, Turku, Finland.

The mass analyzer used in SIMS experiments can be quadrupole, magnetic sector or time-of-flight (Vickerman 2001). In static SIMS, a ToF mass spectrometer is the best choice, because higher mass ranges can be detected. Static SIMS means that the analysis does not destroy the sample surface as the current density of the ion beam is low, in contrast to dynamic SIMS where the sample surface is eroded by the more energetic beam.

SIMS operates under vacuum (Vickerman 2001). During static SIMS analysis, a beam of high-energy ions bombards the surface, their energy being transferred to the atoms of the surface (Fig. 2). The energy is further transferred between the atoms of the sample in a cascade of collisions. Some collisions return to the surface and give the particles there enough energy to escape the surface and become part of the emitted secondary particles. Some of the secondary particles are ionized when leaving the surface. In a static SIMS experiment, the primary ion dose is low ($<1x10^{13}$ ions/cm^2) to ensure that during the analysis less than 1% of the surface atoms or molecules receive an impact and the surface remains virtually undamaged.
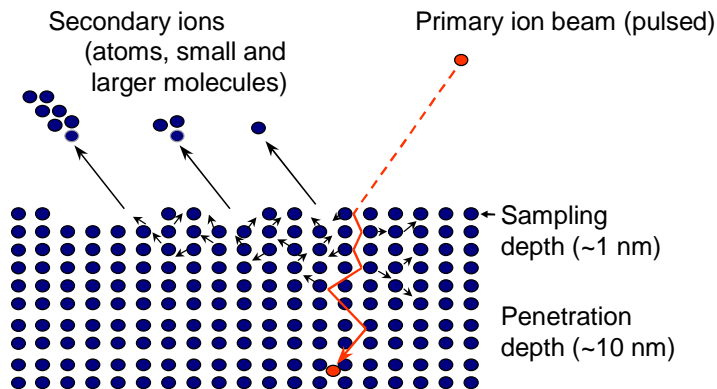
Figure 2. The principle of ToF-SIMS.

Secondary species are emitted from the surface with a range of kinetic energies (Vickerman 2001). The kinetic energy distribution is influenced indirectly by the primary ion energy, angle of incidence and atomicity determining the nature of the collision cascade in the material. Binding of species in the surface, the number of bonds to be broken and the degree to which internal energy can be stored have more direct influences. The kinetic energy distribution of secondary species from metals is typically broad, whereas that of cluster ions is narrower and that of large molecular species from organic materials is usually very narrow.

Surface charging complicates the SIMS analysis of insulating samples such as paper (Vickerman 2001). Bombardment of the surface by an ion beam and emission of secondary electrons causes a rapid increase in surface potential, which raises the kinetic energy of emitted ions beyond the acceptance level of the detector and results in a loss of SIMS spectrum. The problem can be solved by irradiating the sample surface with a beam of low-energy electrons. Normally metal grids are also placed in contact with the sample during analysis to help in charge neutralization.

In ToF analysis, secondary ions are accelerated to a given potential so that all ions have the same kinetic energy. They are then left to drift freely through a field free space before striking the detector. Heavier masses travel more slowly through the flight tube, and thus the lighter masses reach the detector first. The flight time of the ions (t) is defined by equation 1:

$$t = L\left(\frac{m}{2zV}\right)^{1/2}$$

[1]

Where t is the measured flight time, m the mass of ion, z charge of ion, V acceleration potential and L length of flight path. The ToF-SIMS mass spectrum for the ions is generated from the flight time spectrum.

ToF-SIMS analysis yields information in the form of positive (Fig. 3) and negative ion mass spectra (Vickerman 2001). Chemical images of the sample surface can also be obtained (Fig. 4). During imaging, the mass spectrum is recorded at each pixel as the ion beam is rastered over the surface. Images can be obtained from all the secondary ions reaching the detector (Fig. 4, left). In addition, certain masses can be selected and their distribution followed on the sample surface (Fig. 4, right).
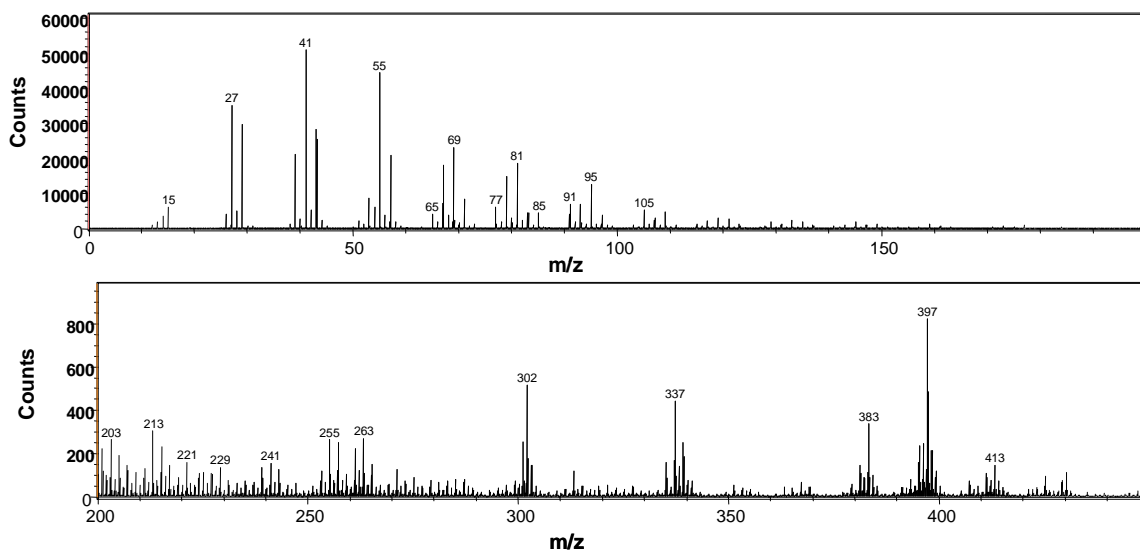
Figure 3. A positive ToF-SIMS spectrum of TMP fibrils in the mass range 0-450 m/z.
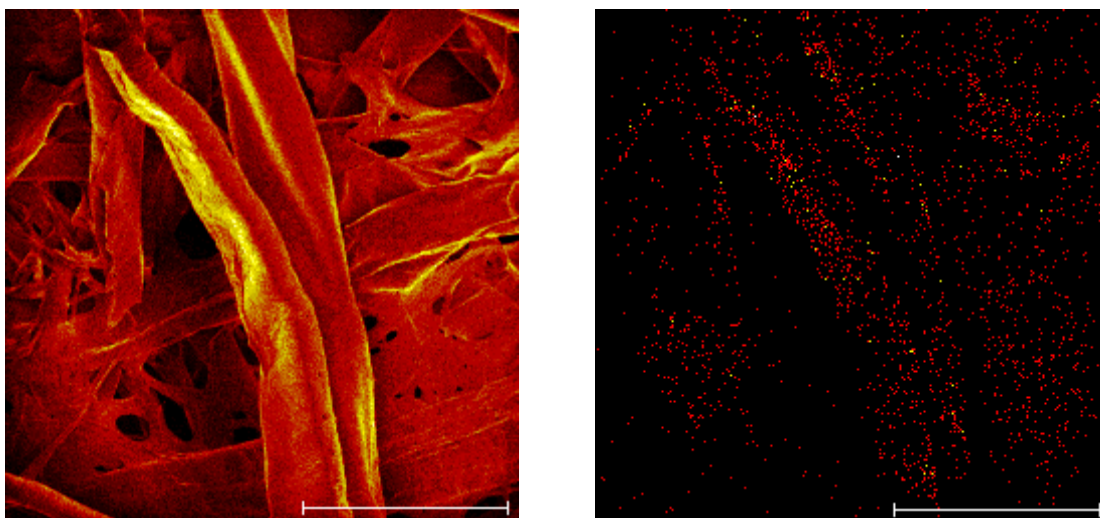
Figure 4. Positive total ion ToF-SIMS image (left) and image of fatty acids (right).

Advantages of ToF-SIMS include detection of all elements, isotope sensitivity, molecular information, low detection limit and parallel detection of all secondary masses (Benninghoven 2001, Schueler 2001). Parallel detection means that the ToF analyzer is always ready to detect any ion mass and does not have to be tuned to a certain mass. However, it does not mean that all ions can be detected simultaneously (Schueler 2001). Both chemical information and information about component distribution can be obtained with ToF-SIMS. No-pretreatment of the sample is usually needed. The only demand is that the sample must withstand high vacuum. Disadvantages include sensitivity loss in

the high mass range and difficult interpretation of the mass spectra. In real-life samples, the surface consists of many different compounds, all of which have their characteristic peaks and fragmentation patterns and which thus generate their own spectra. The resulting ToF-SIMS spectra is therefore the sum of all these spectra (Benninghoven 2001).

3.2 Applications in the pulp and paper research

Brinen et al. (1991) introduced SIMS into pulp and paper research. In this pioneering paper, a SIMS equipped with a quadrupole mass spectrometer was used to study the distribution of inorganic species, namely Ca, Na and Al, on paper surfaces. In the second paper of the series, mapping of organic additives on the paper surface using both quadrupole and ToF mass spectrometers was attempted (Brinen and Proverb 1991). The authors found that using a quadrupole-based SIMS, the distribution of fluorine from a fluorinated surfactant could be analyzed, but with ToF-SIMS, both fluorine and organofluorine fragments could be seen. In addition, the advantages of ToF-SIMS over quadrupole-SIMS included the possibility of making measurements under static conditions, carrying out mass detection and imaging at the same time, simultaneous detection of all ions, detection of higher mass fragments, and higher sensitivity towards both inorganics and organics. Use of a time-of-flight mass spectrometer thus made SIMS a more powerful technique for studying pulp and paper surfaces. With the introduction of the ToF based technique, new applications for SIMS began to appear. Since then, ToF-SIMS has been applied to the study of lignins, wood, mechanical and chemical pulps, papers, surface treatments, coating, printing, etc.

3.2.1 Lignin

The ability of ToF-SIMS to produce interpretable and useful information about lignin structures was tested on spruce and birch milled wood lignins (MWLs) and softwood and hardwood kraft lignins for the first time by Kleen (Kleen 2000a,b). She found that ToF-SIMS gives information about the basic lignin units in softwood and hardwood lignins. Guaiacyl (G) lignin units gave characteristic peaks at m/z 137 and 151 and syringyl (S) units at m/z 167 and 181.

A Japanese research group further studied the use of ToF-SIMS for investigating lignin structure by means of labeling experiments using dehydrogenation polymers (DHPs) and with lignin model compounds (Saito et al. 2005a,b) and confirmed the findings of Kleen (Kleen 2000a,b). They also showed that the guaiacyl peak at m/z 151 consists of two peaks, corresponding to $C_8H_7O_3^+$ and $C_9H_{11}O_2^+$ fragment ions.

3.2.2 Wood

After analyzing beech wood with ToF-SIMS, Japanese researchers (Saito et al. 2005a,b) reported that in their opinion, ToF-SIMS could be used to determine the ratio of syringyl/guaiacyl (S/G) units of lignin in wood and even to determine the S/G ratio in a particular position of a wood sample. Imaging ToF-SIMS could also be used to visualize the distribution of different units in the wood cell wall (Fukushima et al. 2001). Imai et

al. (2005) also studied the heartwood extractives in Sugi (Japanese cedar) with ToF-SIMS. In this work, ToF-SIMS was used to detect any peaks specific to extractives in the heartwood and, when found, to locate them in the heartwood tissue by imaging.

3.2.3 Mechanical and chemical pulps

Early studies of papermaking pulps were performed using SIMS equipped with other mass analyzers than ToF. SIMS equipped with a magnetic sector mass analyzer was used to study the adsorption of aluminum, calcium and silicate on the surfaces of unbleached and bleached PGW (Saastamoinen et al. 1994). SIMS imaging of the elemental distribution on the pulp surface provided information on the location of the adsorption sites in the pulp. Tan and Reeve (1992) used imaging SIMS to study the spatial distribution of non-extractable organochlorine in fully-bleached softwood kraft fibers.

Using ToF-SIMS, Kleen (2000a) studied the surface chemistry of softwood pulps during bleaching and was able to determine the surface metal content and obtain structural information about the surface residual lignin and extractives. The work continued with a structural investigation of residual lignin and extractives on the surface of softwood and hardwood kraft pulps (Kleen 2000b). In this work, characteristic peaks originating from softwood and hardwood lignin as well as typical peaks from extractives were found on the surfaces of extracted samples, possibly indicating residual lignin-extractives complexes. In a study by Kleen and Nilvebrandt (2001), the ability of ToF-SIMS simultaneously to characterize free and esterified fatty acids and their Na and Ca salts was demonstrated. Using this knowledge, Kleen later (2005) analyzed the chemical characteristics of lignin and extractives on hardwood rapid displacement heating (RDH) kraft pulp and during TCF bleaching using ToF-SIMS. In this work, she showed that ToF-SIMS is suitable for direct structural studies of underivatized lignins and extractives on pulp surfaces.

ToF imaging was used to study the metal distribution on the surface of kraft pulp fibers by Mancosky and Lucia (2001). They found that the different bleaching responses of juvenile and mature black spruce kraft pulp fibers may be due to the different metal distributions on their surfaces. In another paper, Mancosky et al. (2002) used ToF-SIMS to evaluate the potential of phytic acid as a chelating agent and discovered that, with the exception of magnesium, metals were homogeneously removed from the fiber surface.

The effect of pulping conditions on the surface chemistry of *Eucalyptus grandis* kraft pulp fibers was studied by means of contact angle measurements, ESCA/XPS and ToF-SIMS (Fardim and Duran 2002). The analysis of surface extractives with ToF-SIMS revealed that calcium and sodium salts of fatty acids persisted on the pulp fiber surface after acetone extraction, indicating their resistance to solvent extraction.

The effect of dielectric discharge, i.e. corona treatment, on the surface of TMP and fully bleached kraft pulps was studied by ToF-SIMS and ESCA/XPS (Vander Wielen and Ragauskas 2003). Imaging ToF-SIMS permitted the topochemistry of acid groups on the pulp surface to be monitored.

Fardim and Holmbom (2005) studied the surface distribution of anionic groups (AGs) on papermaking fibers from chemical, mechanical and chemimechanical pulp by treating the pulps with Mg^{2+} and monitoring these ions using ToF-SIMS. It was found that on mechanical pulps the AGs were located more on fines than on TMP fiber surfaces. After peroxide bleaching, AGs were also found on fibers, probably due to removal of lignin layers and formation of carboxyl groups by lignin oxidation.

Fardim et al. (2005) studied extractives on the fiber surfaces of a bleached birch kraft pulp and a recycled deinked pulp by ToF-SIMS in combination with ESCA/XPS and AFM. ToF-SIMS was used to study the composition of extractives on fiber surfaces and the distribution of extractives was analyzed by ToF-SIMS imaging. Their results showed that the data from ESCA/XPS and ToF-SIMS complement each other and that together these methods are adequate tools for fiber surface characterization.

The surface compositions of elemental chlorine free (ECF) bleached kraft pulp fibers prepared from five different hardwoods were studied using ESCA/XPS and ToF-SIMS by Pascoal Neto et al. (2004). Using ToF-SIMS they were able to detect that fatty acids are the dominant extractives on pulps from certain species, while sterols dominate in other species.

Koljonen et al. (2004) studied the effect of pH on the formation of precipitates on kraft pulp surfaces using ToF-SIMS together with ESCA/XPS and AFM. ToF-SIMS was used to evaluate the relative surface content of lignin and extractives and the amount of metals on pulp surfaces. The authors concluded that the combination of ESCA/XPS, ToF-SIMS and AFM techniques give a comprehensive picture of the chemistry and morphology of the pulp surface.

Kokkonen et al. (2004) used imaging ToF-SIMS to monitor the location of extractives model compounds on the surface of TMP handsheets. The distribution data were combined with ESCA/XPS, attenuated total reflection infrared (ATR-IR) spectroscopy, environmental scanning electron microscope (ESEM) and contact angle measurement data.

3.2.4 Paper

Brinen (1993) continued his pioneering work by studying the presence and distribution of sizing agents on paper surfaces with ESCA/XPS and ToF-SIMS. He concluded that ESCA/XPS can detect the presence of sizing agents on the surface but provides little structural information, while ToF-SIMS can be used to identify the chemical structures of the sizing agents and to study their spatial distribution on the paper surface. The cause of sizing difficulties in sulfite paper was studied with a combination of ToF-SIMS and paper chromatography (Brinen and Kulick 1996) and ESCA/XPS (Brinen and Kulick 1995). SIMS imaging showed the presence of high mass ions on the surface of the paper, and ToF-SIMS and chromatography together were used to identify these desizing chemicals as pitch. In studying the effect of hydrolyzed alkenyl succinic acid (ASA) on sizing in calcium carbonate–filled paper, Wasser and Brinen (1998) used ToF-SIMS to confirm the chemical changes in hydrolyzed ASA. SIMS has also been used to solve other paper surface defects such as fish eyes and brown specks (Kulick and Brinen 1996).

Istone (1994) described the use of ESCA/XPS and ToF-SIMS to characterize defects in paper due to changes in surface chemistry. Three different problems were studied: poor polyethylene adhesion in milk cartons, black streaks on xerographic paper and yellow spots on lithographic paper.

Zimmerman et al. (1995b) used ToF-SIMS to solve two real-life paper-related problems. Two papers, one giving a high-quality print and the other a mottled print were compared. ToF-SIMS spectra and images revealed that the reason for mottling was uneven distribution of calcium on the paper surface. Uncoated adhesive labels were also analyzed with ToF-SIMS to determine the nature and cause of surface contamination. The contamination causing spotting turned out to be PDMS, which probably originated from the labels' release sheet. ToF-SIMS was also used to directly quantify alkyl ketene dimer (AKD) size on a paper surface after establishing a calibration curve with papers of known AKD loadings (Zimmerman et al. 1995a).

The chemical changes taking place on cellulose filter paper during N_2 plasma treatment were studied using ToF-SIMS and ESCA/XPS (Deslandes et al. 1998). With ToF-SIMS, various functionalities containing nitrogen could be detected on the paper surface, even after a short period of plasma exposure.

The distribution of rosin sizing agent on the paper surface was studied with both unlabelled and fluorine-labeled samples using electron-probe micro analysis (EPMA), ESCA/XPS and ToF-SIMS (Ozaki and Sawatari 1997). It was found that unlabelled samples were better suited for ToF-SIMS analysis. The authors also found no correlation between the rosin content in the handsheet and the secondary ion intensity measured with ToF-SIMS. The study of rosin sizing agent was also attempted by labeling it with osmium tetroxide (OsO_4) in the gas phase and analyzing the distribution with ESCA/XPS and ToF-SIMS (Sawatari et al. 1999). The intensities of negative secondary ions did not properly correlate with the content of rosin, but there was a correlation between positive secondary ion intensity and rosin content.

Ozaki and Sawatari (Ozaki and Sawatari 2002) were interested in the distribution of rosin size on the surface of hardwood bleached kraft pulp handsheets. They used imaging ToF-SIMS and a fragment ion of 128 amu ($C_7H_{12}O_2^+$) to locate the rosin size.

ToF-SIMS was used to complement and explain the results given by ESCA/XPS on the depth of penetration of styrene-maleic imide resin (SMA I) in the z-direction of paper (Valton, Sain et al. 2003). Depth profiling was accomplished using cross-sections of paper and imaging the characteristic peaks of this resin.

Lipponen et al. (2004) used imaging ToF-SIMS for comparison of a method developed for determining starch penetration in a surface-sized fine paper. Starch penetration was studied by monitoring the location of lithium ions originating from $LiCl_2$ added to starch during surface sizing.

The suitability of various surface-sensitive analysis techniques for studying the distribution of papermaking chemicals on multi-use papers was evaluated by Fardim and Holmbom (2005). The analysis techniques compared were ToF-SIMS, ESCA/XPS, field

emission (FE) SEM and energy dispersive X-ray spectrometry (EDS). The authors concluded that the surface distribution of paper and coating chemicals could only be assessed by ToF-SIMS. The other techniques either lacked chemical information (FE-SEM) or had poor lateral resolution (EDS and ESCA/XPS). The intensity of secondary ions originating from papermaking chemicals during a ToF-SIMS experiment was increased after coating the paper sample with a layer of Au-Pd, which led to more detailed images.

Matsushita et al. (2005) used ToF-SIMS to study the behavior of rosin glycerin ester in rosin sizes under different papermaking conditions. A deuterium-labeled rosin glycerin ester was synthesized and its location in bleached hardwood kraft pulp handsheets determined using imaging ToF-SIMS by following the deuterium ion peak.

Koivula et al. (2006) applied ToF-SIMS to the study of pigment particle surfaces. Using ToF-SIMS, they were able to detect dispersant agents on the surface of clay and calcium carbonate pigments and to study their lateral distributions.

3.2.5 Print

Pachuta and Staral (1994) used ToF-SIMS to study different pen inks and printed patterns on paper. They found ToF-SIMS to be a rapid method for the differentiation of colorants, given that colorant systems produce characteristic and abundant secondary ions in the experiment.

Pinto and Nicholas (1997) used imaging ToF-SIMS for the study of different ink jet media. With ToF-SIMS, they determined the extent of ink penetration in model coatings and commercial media and drew conclusions about the ink jet dye binding capacities of different media.

Dynamic SIMS and ToF-SIMS together with ESCA/XPS were used for z-direction analysis of the chemical composition of an ink film printed onto coated paper and to study the distribution of ink components (Dalton et al. 2002). Gentle ion etching through the ink film was used to obtain depth profiling. Using ToF-SIMS, it was difficult to quantify composition as a function of the depth and dynamic SIMS depth profiling was used instead.

The distribution of water-based gravure ink on coated papers has been studied using EPMA, ESCA/XPS and ToF-SIMS (Ozaki and Uchida 2002). ToF-SIMS imaging was used to study the spatial distribution of ink pigment and vehicle on the coated paper surface. The results showed that the distribution of vehicle was different from that of the pigment and that the vehicle spread more widely than the pigment on the coated paper surface.

ToF-SIMS was used to study ink and coating formulations on ink-jet paper and photopaper surface (Sun et al. 2004). The penetration and distribution of these components in the z-direction of the paper were determined by analyzing paper cross-sections with imaging ToF-SIMS. Principal component analysis was applied to the imaging data to improve the chemical contrast between the ink, coating and paper layers. The same methodology was used to study the distribution of ink components (vehicle, binder,

modifier and pigment) both on the surface and in the z-direction of coated ink-jet and photopapers (Sodhi et al. 2005).

4   OTHER METHODS

4.1 Electron spectroscopy for chemical analysis/X-ray photoelectron spectroscopy (ESCA/XPS)

ESCA/XPS is based on the photoelectric effect: when a material is irradiated with x-rays, the electrons in the material can be emitted if the energy of the incoming photons is larger than the energy holding the electrons in their orbital (Istone 1995). The kinetic energies of the emitted photoelectrons depend on their binding energies:

$$E_k = hv - E_b \hspace{4cm} [2]$$

Where E_k is the kinetic energy of the photoelectron, hv the energy of the X-ray and E_b the binding energy of the electron in its orbital. In the ESCA/XPS analysis, the kinetic energies of the emitted electrons are measured.

The electrons generated by the photoelectric effect generally have low kinetic energies and cannot travel large distances in the matter (Istone 1995). This leads to two typical features of the ESCA/XPS technique: firstly, a high vacuum is needed to avoid the scattering of the emitted electrons and secondly, ESCA/XPS is a surface sensitive analysis method, since only electrons in the surface layer have enough energy to escape from the surface.

For pulp and paper samples, a monochromator that allows only x-rays of given wavelengths to reach the sample, and neutralizer or flood gun that prevents charging of the sample surface are used (Istone 1995). The analysis depth of the instrument can be varied by varying the acceptance angle of the analyzer lens. The lens also applies a retard voltage to the incoming electrons so that the electrons have the correct energy to enter and be separated by the analyzer.

Photoelectrons generated by an element can be seen as discrete lines or peaks in the ESCA/XPS spectrum (Istone 1995). The predominant peaks in the ESCA/XPS spectrum are due to electrons emitted from inner shells and the positions of these peaks are used to identify the elements present on the surface. As the spectrum in Fig. 5 shows, the dominant elements on the surface of TMP are oxygen and carbon.
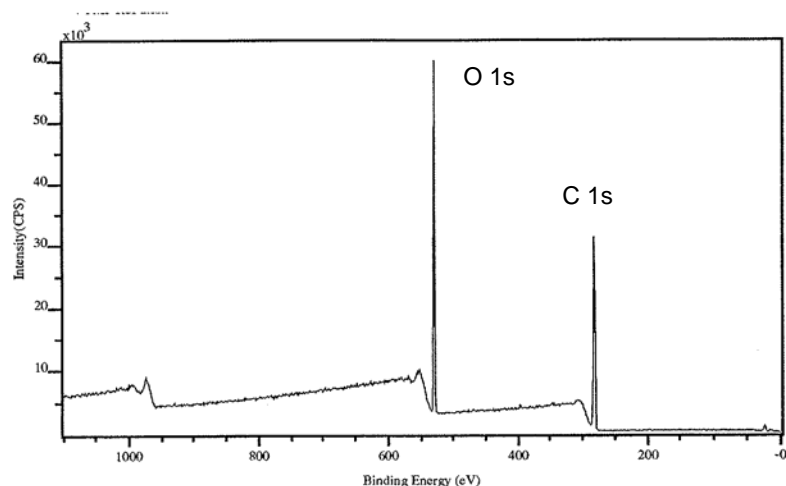
Figure 5. Survey ESCA/XPS spectrum of TMP.

In order to obtain information about the chemistry of the elements on the surface and perform quantative analysis, high-resolution spectra are needed (Istone 1995). To obtain these, a series of narrow (~20 eV) regions are scanned at high resolution around each peak of interest. In high-resolution spectra, information about chemical shifts can be found. Chemical shifts result from the influence of the neighboring atoms to the attraction between the nucleus and the core electrons in the atom being studied. For example, carbon atom bound to a more electronegative oxygen would have some of its electrons attracted to oxygen and there would be a greater attraction between the remaining electrons and increase in binding energy. The carbon 1s peak is thus divided into four distinctive peak in the high-resolution spectrum of TMP (Fig. 6, right): peaks originating from no bonds to oxygen (C1), from one bond to oxygen (C2), from two bonds to oxygen (C3) and from three bonds to oxygen (C3).
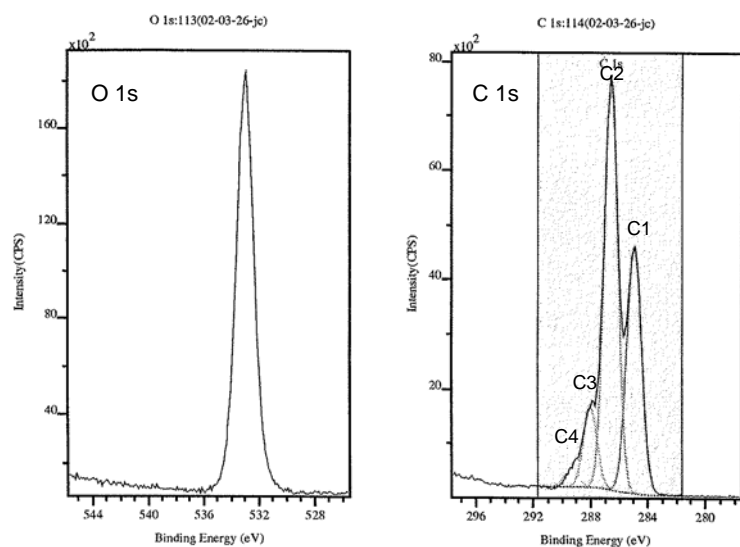
Figure 6. High-resolution ESCA/XPS spectra of O 1s (left) and C 1s regions from TMP.

4.2 Atomic force microscopy (AFM)

AFM is based on the measurement of force between a sharp tip and the sample (Hanley and Gray 1995). The force is measured as an elastic deflection of the cantilever supporting the tip by a sensor. For a cantilever with a given spring constant, the force on the tip can be calculated from Hooke's law:

F=-kZ   [3]

Where Z is the displacement of the cantilever and k a spring constant. AFM measurements can be done using eiher non-modulated or modulated techniques (Hanley and Gray 1995). With non-modulated techniques, the displacement of the cantilever on contacting the surface is used directly as z the data, whereas with modulated techniques, the cantilever deflection is kept constant with a feedback loop by moving the piezo in the z direction, and the signal from the feedback loop is used as the z data.

Three-dimensional height images of the sample surface can be created with AFM by scanning the tip mounted on elastic cantilever over the surface (Hanley and Gray 1995). The interatomic forces between the sample surface and the tip cause the cantilever to deflect either towards the surface (attraction) or away from the surface (repulsion). These forces are detected by monitoring either the deflection of the cantilever or the change in the z-piezo position, which is used to compensate the cantilever deflection.

AFM has different operating modes, differing in their contact between the tip and the sample surface (Hanley and Gray 1995, Moss and Groom 2002). In contact force microscopy, the tip is brought to a distance within a few ångstroms of the sample surface. The repulsive forces between their respective atoms cause the cantilever to deflect, which is sensed with a laser beam and a position-sensitive photodiode detector. In non-contact microscopy, the cantilever is modulated at or near its resonance frequency, causing a low amplitude oscillation in the tip. This vibrating tip is then lowered toward the sample surface until it begins to encounter van der Waals forces, typically 20-200 Å from the sample surface. There is a force gradient acting on the tip and the interaction with the surface causes the effective spring constant of the cantilever to change. The sample can be imaged using a feedback loop to keep the resonance fixed, which allows profiling at constant value of the force gradient.

AFM tapping mode is a variation of the modulated non-contact force microscopy, and most of the research on cellulosic fibers has been done in tapping mode, due to minimal damage to the sample surface and the images of high spatial resolution acquired (Hanley and Gray 1995, Moss and Groom 2002). In the tapping mode, the cantilever oscillates at or near its resonance frequency and there is a brief contact between the tip and the sample surface during each oscillation. The tip-surface contact modifies the amplitude of the oscillation and a feedback loop is used to image the surface at a set modified oscillation amplitude.

Phase detection is done with tapping mode AFM by monitoring the phase lag of the cantilever oscillation relative to the oscillation of the drive piezo, which in part indicates the surface adhesion or viscoelastic properties of the sample (Hanley and Gray 1995, Moss and Groom 2002). Phase imaging can be used to differentiate between various components on the surface of wood or pulp fibers, such as lignin and cellulose, based on the degree of the phase shift. It can also be used to identify surface contaminants. The images resulting from phase imaging have higher contrast than height images, since phase detection is sensitive to surface topography.

4.3 Field emission scanning electron microscopy (FE-SEM)

In scanning electron microscope, accelerated primary electrons form a beam that is scanned across the sample surface (de Silveira et al. 1995). The primary electrons have a number of interactions with the atoms of the sample, leading to the scattering of the electrons. The interactions may be either elastic or inelastic in nature. Elastic scattering results from the collision of primary electrons with the nuclei of the atoms in the sample with negligible transfer of kinetic energy, and gives rise to backscattered electron (BE) signal. Inelastic scattering transfers energy from the beam electrons to the atoms of the sample, thus decreasing the kinetic energy of the primary electrons. This interaction leads to the ejection of loosely bound electrons of low energy (0-50 keV), referred to as secondary electrons (SE), which originate from shallow sampling depth. In addition to secondary electrons, inelastic scattering also leads to the generation e.g. characteristic x-rays. In conventional SEMs, there are usually detectors for the secondary and backscattered electrons and possibly for x-rays. Secondary electrons originating from the top layers of the sample provide information of its topography, whereas backscattered electrons are produced deeper in the sample and give information of the elemental composition.

Resolution of the electron microscope depends on the diameter of the primary electron beam and thus on the type of the electron source. The image resolution can be improved by decreasing the electron-probe size without causing a loss of current in the probe. This can be accomplished by increasing the electron gun brightness (Goldstein et al. 1992). In conventional SEMs, the electrons are produced by heating a tungsten filament, whereas in FE-SEMs, the electron source is a wire of single-crystal tungsten forming a sharp tip point. The brightness of the tungsten hairpin filament in the conventional SEM is 105 A/cm^{2}sr and the source size 30-100 µm, whereas the brightness of the FE electron gun is 10^8 A/ cm^{2}sr and the source size is less than 5 nm (Goldstein et al. 1992). In FE-SEM, a strong electric field is concentrated into the tip of small radius to release the electrons and high-resolution images can be obtained. FE-SEMs are suitable for high magnifications and working with low acceleration voltages, making them excellent tools for surface sensitive imaging.

5 EXPERIMENTAL

5.1 Materials

5.1.1 Pulps

The pulp samples used in this study were unbleached Norway spruce (*Picea abies*) mechanical pulps obtained from Finnish or Swedish pulp mills, pulps produced in pilot scale by refining Norway spruce wood (*Picea abies)* chips at different specific energy consumptions, mill pulps bleached under laboratory conditions, and enzymatically treated thermomechanical pulps. All the pulps are described in Table 1.

For the refining study, thick-walled Norway spruce (*Picea abies*) from a slow-growth forest stand approximately 60 years old was used as raw material. Refining was carried out on the pilot scale at KCL. A detailed description of the refining experiments can be found in Paper III.

TMP and CTMP were peroxide-bleached in the laboratory. TMP was also bleached with dithionite in the laboratory. The bleaching experiments are described in Paper IV.

The enzymatic treatments were performed at VTT using mill TMP. The pulp was treated with six different enzymes: xylanase, mannanase, lipase, laccase, pectinase and protease. The enzymatic treatments are described in Paper V.

Table 1. Notation, source and properties of pulp samples*.

Notation	Description	Properties
Peeled pulp (Paper I)		
TMP	Taken after the 2nd refiner	CSF 150 ml
Unbleached pulps		
TMP (Paper II)	Taken after 2nd refiner	CSF 124 ml, d.w. 55%, BMcNett +14 28.6%, -200 24.7%
CTMP (unpubl.)	Taken from 1st refiner	CSF 627 ml, d.w. 46.4%, BMcNett +14 40.5%, -200 16.6%
GW (unpubl.)	Taken from disc filter	CSF 24 ml, d.w. 9.5%, BMcNett +14 0.5%, -200 45.1%
PGW (unpubl.)	Taken from disc filter	CSF 89 ml, d.w. 21.1%, BMcNett +14 10.8%, -200 35.2%
Refined pulps (Paper III)		
A1	Pilot refined, taken after 1st refining stage, SEC 1.55 MWh/t	CSF 340 ml, BMcNett +14 36.8%, -200 18.4%
A2	Pilot refined, taken after 2nd refining stage, SEC 2.44 MWh/t	CSF 122 ml, BMcNett +14 30.5%, -200 24.1%
B1	Pilot refined, taken after 1st reject refining stage, SEC 3.94 MWh/t	CSF 100, BMcNett +14 33.3%, -200 17.9%
B2	Pilot refined, taken after 2nd reject refining stage, SEC 4.44 MWh/t	CSF 60 ml, BMcNett +14 38.1%, -200 18%
B3	Pilot refined, taken after 2nd reject refining stage, SEC 4.65 MWh/t	CSF 50 ml, BMcNett +14 37.3%, -200 17.7%
B4	Pilot refined, taken after 2nd reject refining stage, SEC 4.88 MWh/t	CSF 37 ml, BMcNett +14 35.8%, -200 19.9%
Bleached pulps (Paper IV)		
TMP-P	Laboratory peroxide-bleached TMP	CSF 180 ml, d.w. 17.8%, BMcNett +14 28.8%, -200 26.0%, ISO% 75.0
CTMP-P	Laboratory peroxide-bleached CTMP	CSF 625 ml, d.w. 15.9%, BMcNett +14 40.3%, -200 17.2%, ISO% 75.5
TMP-Y	Laboratory dithionite-bleached TMP	CSF 176 ml, d.w. 4%, BMcNett +14 28.6%, -200 26.3%, ISO% 68.7
Enzymatically treated pulps (Paper V)		
Reference	Reference treated TMP, no enzyme addition	CSF 144 ml, BMcNett +14 29.2%, -200 27%
Xylanase	TMP treated with xylanase	CSF 164 ml, BMcNett +14 28.5%, -200 26.2%
Mannanase	TMP treated with mannanase	CSF 216 ml, BMcNett +14 27.7%, -200 23.2%
Lipase	TMP treated with lipase	CSF 131 ml, BMcNett +14 32.2%, -200 22.2%
Laccase	TMP treated with laccase	CSF 160 ml, BMcNett +14 31%, -200 23.1%
Pectinase	TMP treated with pectinase	CSF 153 ml, BMcNett +14 28.1%, -200 24.5%
Protease	TMP treated with protease	CSF 147 ml, BMcNett +14 30.8%, -200 24%

*CSF=canadian standard freeness, d.w.=dry weight, BMcNett = fractionation performed by BauerMcNett, +14 = fiber fraction, -200 = fines fraction, ISO% = ISO brightness and SEC = specific energy consumption.

5.1.2 Isolated pulp fractions: fibers, fibrils and flakes

From the TMP used for the peeling studies, fines were first separated from the pulp suspension (2% conc.) by filtration through a 100 μm nylon cloth. The separated fibers were then subjected to gentle mechanical peeling (20 000 rpm, 4.5% conc.) in a British standard disintegrator. The material released was removed by filtration through a nylon cloth. The isolated fractions (fines, peeled material and peeled fibers) were freeze-dried for further analysis (Paper I).

For the separation of fibers and fines from the other pulps (unbleached pulps, refined pulps, bleached pulps and enzymatically treated pulps), a dynamic drainage jar (DDJ) equipped with a 200 mesh (76 μm) wire and propeller stirring was used. A detailed description of the separation procedure can be found in Paper II. Image analysis was used to evaluate the success of the separation procedure by measuring the apparent content of fibrillar material (%) in the enriched fractions of fibrils and flakes (Table 2). The result for the fractionation of TMP was also evaluated by light microscopy and SEM (Paper II).

Table 2. Apparent fibril content (%) of isolated fibril and flake fractions*.

Pulp	Enriched fibrils	Enriched flakes
Unbleached pulps		
TMP	86	18
CTMP	70	9
GW	71	42
PGW	70	35
Refined pulps		
A1	81	21
A2	84	8
B1	84	11
B2	81	11
B3	83	11
B4	80	11
Bleached pulps		
TMP-P	85	19
CTMP-P	85	15
TMP-Y	86	27
Enzymatically treated pulps		
Reference	80	13
Xylanase	58	12
Mannanase	53	15
Lipase	68	16
Laccase	63	16
Pectinase	71	17
Protease	78	15

*For sample abbreviations, refer to Table 1.

5.1.3 Pulp sheets

For ESCA/XPS, ToF-SIMS and AFM analysis, small sheets were prepared from the pulps and fiber, fibril and flake fractions. The sheets were made in a glass funnel on a 20 μm nylon screen, dried between blotters and stored in a freezer. For ESCA/XPS analysis, part

of each sheet was extracted with acetone in a Soxhlet apparatus for 4 h using 120 ml of acetone. After extraction, the sheets were dried between blotters and stored in a freezer until needed.

5.1.4 Model compounds for ToF-SIMS analysis

Interpretation of ToF-SIMS spectra required the analysis of model compounds. A list of the model compounds used is presented in Table 3. The purity of the model compounds was not tested.

Table 3. Model compounds used for the interpretation of ToF-SIMS spectra.

Compound	Description	Source
Lignin		
Spruce MWL Spruce TMP MWL Spruce TMP fines MWL	MWL isolated from spruce wood, spruce TMP and spruce TMP fines, respectively	In-house preparation (KCL) according to the slightly modified Björkman method (Björkman 1956)
Cellulose		
Filter paper Avicell DCM-extracted cellulose		Schleicher&Schuell Merck In-house preparation (KCL)
Hemicelluloses		
Mannan	Galactoglucomannan from Chrommager I Galactomannan from locust bean gum Glucomannan from spruce sulfite pulp Ivory nut mannan	In-house preparations (KCL) Obtained from VTT
Xylan	Pine xylan purified by dialysis Glucuronoxylan Arabinoxylan	In-house preparations (KCL)
Galactan	Arabinogalactan from larch	In-house preparation (KCL)
Pitch		
TMP acetone extract	Acetone-extracted from TMP	In-house preparation (KCL) Soxhlet extracted according to SCAN-CM 49:93 (1993)
Palmitic acid	Sat. fatty acid	Sigma
Heptadecanoic acid	Sat. fatty acid	Fluka
Stearic acid	Sat. fatty acid	Fluka
Oleic acid	Unsat. fatty acid	Obtained from STFI
Linoleic acid	Unsat. fatty acid	Obtained from STFI
Linolenic acid	Unsat. fatty acid	Fluka
Arachidic acid	Sat. fatty acid	Fluka
Eicosatrienoic acid	Unsat. fatty acid	Sigma-Aldrich
Behenic acid	Sat. fatty acid	Fluka
Tetracosanoic acid	Sat. fatty acid	Fluka
1-Eicosanol	Fatty acid alcohol	Fluka
1-Docosanol	Fatty acid alcohol	Fluka
Tripalmitin	Triglyceride	Sigma
Triolein	Triglyceride	Fluka
Tristearin	Triglyceride	Sigma
Dehydroabietic acid	Resin acid	Helix Biotech Corp.
Abietic acid	Resin acid	Fluka
Ultrasitosterol	Mixture of sterols	UPM-Kymmene
Steryl esters	Mixture of steryl esters	Raisio Chemicals
Squalene	Hydrocarbon	Fluka

5.2 Methods

5.2.1 ToF-SIMS

The instrument used was a PHI TRIFT II time-of-flight secondary ion mass spectrometer from Physical Electronics. The measurements were made at Top Analytica Oy Ltd, Turku, Finland. ToF-SIMS spectra in positive and negative ion modes were acquired using a Ga liquid metal ion gun with 15 keV primary ions in bunched mode over the mass range 2-2000 m/z. The primary ion current was 600 pA, time per channel 0.138 ns, analysis area 200x200 μm^2 and acquisition time 5 minutes. Analytical charge compensation was used for insulating the pulp samples. The calculated ion dose was $2.7 \cdot 10^{11}$ /cm^2, which ensured static conditions during the acquisition. Three replicate runs were made from each sample. Peak identification in ToF-SIMS spectra was based on model compound analysis. ToF-SIMS images were acquired with 25 keV primary ions in unbunched mode from an analysis area of 250x250 μm^2. Otherwise the conditions were the same as during the acquisition of spectra.

Parts of the positive ToF-SIMS spectra of spruce MWL and spruce TMP MWL are shown in Fig. 7. The spectra are shown for mass to charge ratios (m/z) from 100 to 200, which is the most interesting area for detecting the molecular fragments of lignin and carbohydrates. For pulp samples, mostly fragments of hydrocarbons can be seen in the mass range below 100 m/z (CH$_2$, CH$_3$ etc., Fig. 3). The metals present in the pulp (e.g., Na, Ca and Al) can also be detected here. Usually, their peak intensity is small compared to the peak intensity coming from hydrocarbons, so that magnification of the spectrum would be needed to detect them. Peaks representing different functionalities in compounds (e.g., HO-, H$_3$CO- and -COO$^-$) can also be seen in this region. However, the compounds or fragments mentioned above are very common in many materials, so that this region is seldom of use in the study of organic compounds on pulp surfaces.
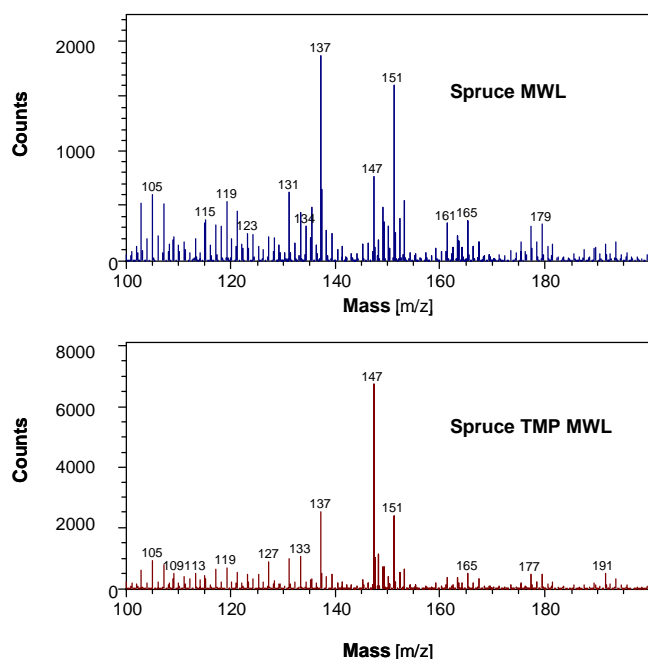
Figure 7. ToF-SIMS spectra of spruce MWL and spruce TMP mill wood lignin.

In the spectra shown in Fig. 7, peaks characteristic of spruce lignin can be seen at 137 and 151 m/z. These represent the guaiacyl units in lignin. The peak at 137 m/z corresponds to the guaiacyl lignin unit, which has a –CH_2 group in the α position and the peak at 151 m/z to a guaiacyl unit with –C=O in the α position. These peaks have been identified earlier (Kleen 2000b; Saito et al. 2005a). The large peak at 147 m/z in the lower spectrum probably originates from contamination by PDMS or phthalates (Reich 2001).

Parts of the positive ToF-SIMS spectra of cellulose, mannan and xylan are shown in Fig. 8. All these spectra contained peaks at 115, 127, 133 and 145 m/z. Since the peaks at 115 and 133 m/z were relatively more intense in the xylan spectra, they were interpreted to originate from pentosaccharides, while the peaks at 127 and 145 m/z were interpreted to originate from hexosaccharides. However, surfaces containing carbohydrates, especially cellulose, were easily contaminated and it was difficult to find peaks characteristic of polysaccharides. The large peaks in the spectra in Fig. 8 at 147 and 149 m/z are both characteristic of phthalates and peak at 147 m/z also of PDMS.
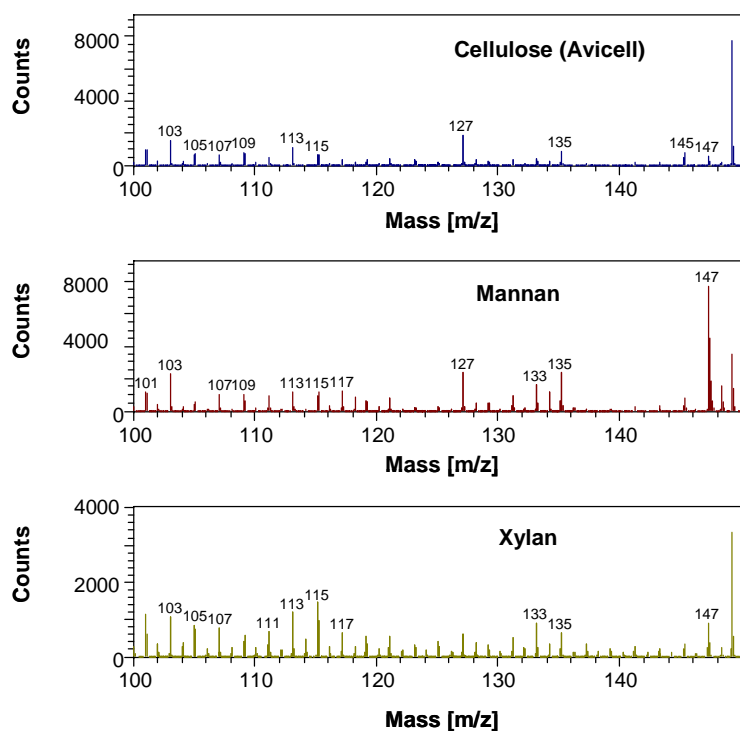
Figure 8. Part of the positive ToF-SIMS spectra of cellulose (Avicell), mannan and xylan.

Peaks characteristic of wood extractives are usually seen in the mass to charge ratio from 230 m/z to 650 m/z. Some examples of the ToF-SIMS spectra of model compounds representing the most common extractives in Norway spruce are shown in Figs. 9 and 10. As the ToF-SIMS spectra of triolein shows (Fig. 9), triglycerides are fragmented in the ToF-SIMS experiment and contribute to the peak intensity of free fatty acids. In addition, triglycerides give peaks at around 600 m/z representing the fragmented di-form and a peak at 339 m/z for the mono-form. The peak 265 m/z represents the fragmented free fatty acid form, and the same peak is seen in the ToF-SIMS spectrum of oleic acid. Thus with ToF-SIMS, it is not possible to fully distinguish between the esterified and free fatty acids. However, the presence of peaks at around 600 m/z and at 339 m/z indicates that the sample contains triglycerides. The secondary ions from free fatty acids can be seen in the positive ToF-SIMS spectra as either protonated molecular ions [M+H]$^+$ or as molecular ions having lost one hydroxyl group [M-OH]$^+$. An example of this is palmitic acid, which has a molecular mass of 256 Da and characteristics peaks at 257 (256+1) m/z and 239 (256-17) m/z (Fig. 9).
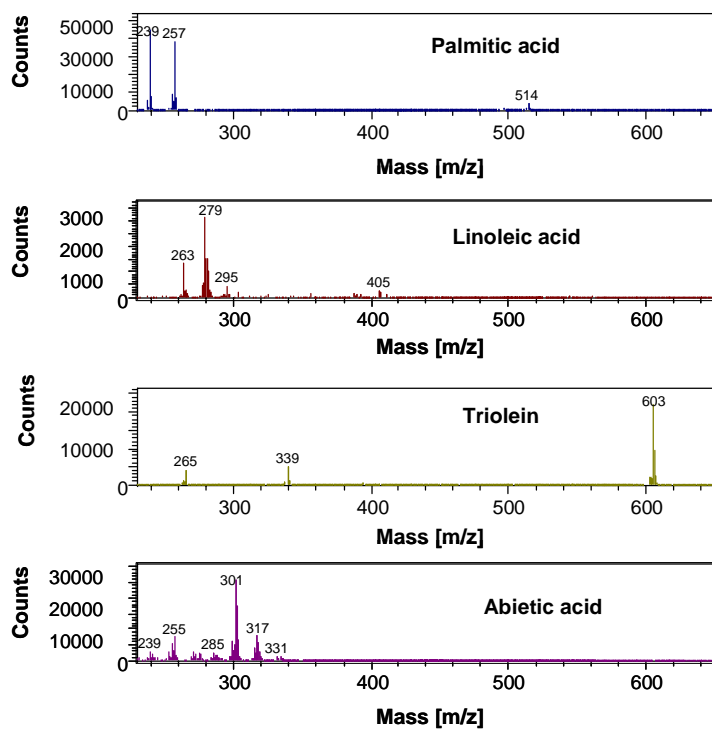
Figure 9. Part of the positive ToF-SIMS spectra of model compounds for wood extractives: palmitic acid (Mw 256 Da), linoleic acid (Mw 280 Da), triolein (Mw 885 Da) and abietic acid (Mw 302 Da).

Parts of the positive ToF-SIMS spectra of the mixture of steryl esters and ultrasitosterol are shown in Fig. 10. Both compounds have characteristic peaks at 381, 383, 397 and 411 m/z. Steryl esters also have a characteristic peak at 425 or 429 m/z. The peak at 397 m/z probably originates from sitosterol [M-OH]$^+$ and the peak at 383 m/z from campesterol [M-OH]$^+$.

Fig. 8 shows parts of the positive ToF-SIMS spectra of acetone extracts of TMP and CTMP. The spectra contain peaks from all the above mentioned extractives groups: from fatty acids and triglycerides at 257, 285, 313, 337, 369 and 599 m/z, from resin acids at 302 m/z and from sterols and steryl esters at 383, 397, 411 and 425 m/z.
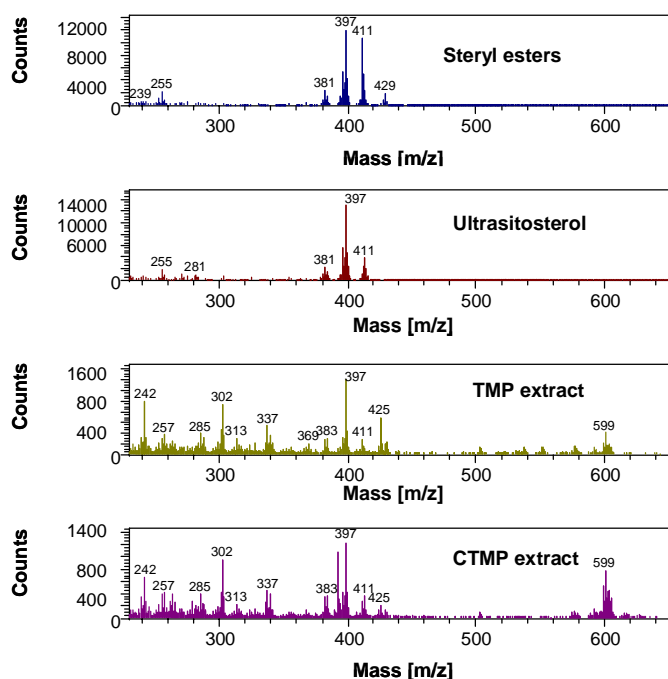
Figure 10. Parts of the positive ToF-SIMS spectra of steryl esters, ultrasitosterol and acetone extracts of TMP and CTMP.

Model compound analysis was also performed in the negative ToF-SIMS mode, and negative ToF-SIMS spectra of the samples were used for the analysis of fatty and resin acids in Papers I, II and III, in which more details can be found. Negative peaks usually correspond to molecular ions having lost one hydrogen atom [M-H]⁻. However, in Papers IV and V, the analysis of extractives was based solely on positive ToF-SIMS spectra to allow better comparison of the different extractives groups. Additional peaks were then selected for the analysis in order to improve its accuracy. The results shown in Papers I, II and III are therefore not directly comparable with those presented in Papers IV and IV.

All the spectral peaks used in the ToF-SIMS analysis of samples are summarized in Table 4. The Papers in which the peaks were used are given in parenthesis. Some extractives compounds could not be determined, because no characteristic peaks were found. In the case of lignin, cellulose and hemicellulose, negative spectra were found not to be of interest.

Table 4. Characteristic peaks for different pulp components*.

Compound	Characteristic peaks in positive spectra (m/z)	Characteristic peaks in negative spectra (m/z)
Lignin		
Guaiacyl units	137, 151 (I, III, IV, V)	n.a.
Methoxyl groups	31 (I, IV)	n.a.
Aromatic units	77 (I)	n.a.
Lignin chromophores	177, 178, 179 (IV)	n.a.
Cellulose		
Hexosaccharides	127 (I, IV, V)	n.a.
Hemicelluloses		
Mannan	127, 145 (IV, V)	n.a
Xylan	115, 133 (IV, V)	n.a.
Fatty acids		
Palmitic acid	239, 257 (IV, V)	255 (I,II,III)
Heptadecanoic (methyl-hexadecanoic) acid	253, 271 (IV, V)	269 (I, II, III)
Stearic acid	267, 285 (IV, V)	283 (I, II, III)
Oleic acid	265, 283 (IV, V)	281 (I, II, III)
Linoleic acid	263, 281 (IV, V)	279 (I, II, III)
Linolenic acid (pinolenic acid)	261, 279 (IV, V)	277 (I, II, III)
Arachidic acid	295, 313 (IV, V)	311 (II, III)
Eicosatrienoic acid	n.a.	305 (II, III)
Behenic acid	323, 341 (IV, V)	339 (II, III)
Tetracosanoic acid	351, 369 (IV, V)	367 (II, III)
Fatty alcohols		
1-Eicosanol	n.a.	n.a.
1-Docosanol	n.a.	n.a.
Triglycerides		
Tripalmitin	313, 551 (II, III, IV, V)	255
Triolein	339, 603 (II, III, IV, V)	281
Tristearin	341, 607 (II, III, IV, V)	283
Triglycerides of other fatty acids	327 (II, III), 335 (II, III), 337 (II, III), 575, 595 (II, III), 599 (II, III), 600, 601, 602 (IV, V)	
Resin acids		
Dehydroabietic acid	299, 300, 301, 302, 303 (IV, V)	299 (I, II)
Abietic acid	299, 300, 301, 302, 303 (IV, V)	301 (I, II)
Steroids		
Ultrasitosterol	383, 397 (I, II), 414, 429	413
Steryl esters	383, 397, 411, 425/429 (I, II, IV, V)	411, 425
Hydrocarbons		
Squalene	n.a.	n.a.

* n.a. = not analyzed

In order to obtain semi-quantitative information about the surface compounds, the peaks of interest shown in Table 4 were integrated and normalized either to the intensities of some other known peaks or to the total intensity of the spectrum. This method does not provide fully quantitative results, but allows samples to be compared. The standard deviation between the integrated and normalized values was usually well below 10%.

5.2.2 ESCA/XPS

The ESCA/XPS analyses were performed with an AXIS 165 high-resolution electron spectrometer from Kratos Analytical. The measurements were made at the Center of Chemical Analysis, Helsinki University of Technology, Espoo, Finland. Sample sheets were measured before and after acetone extraction. Small samples of the sheets were attached to the sample holder without adhesive and evacuated overnight in order to stabilize the water content.

The measurements were made using monochromatic Al Kα irradiation (12.5 kV, 8 mA). Both survey scans in the range 0-1100 eV (1 eV step, 80 eV analyzer pass energy) and high-resolution spectra of C1s and O1s regions (0.1 eV step, 20 eV pass energy) were recorded at three different locations for each sample. The area of analysis was about 1 mm^2 and the depth of analysis in the range 2-10 nm. The insulating sample surfaces were neutralized during the measurement with low-energy electrons. The binding energies were calibrated after the measurements using the C-C component of C 1s signal as an internal standard. Experimental points with asymmetric high-resolution peaks (indicating surface charging) were discarded and re-recorded.

In the high-resolution spectra, carbon atoms were divided into four categories based on the number of bonds with oxygen (C-C, C-O, O-C-O and O-C=O). The apparent surface coverage (Φ) of lignin and extractives was calculated from the averaged C-C percentages in high-resolution C 1s spectra, measured before $(C-C)_{before\ extraction}$ and after acetone extraction $(C-C)_{after\ extraction}$, using equations 2 and 3:

$$\Phi_{lignin}(\%)=[(C-C)_{after\ extraction} - a)]b \qquad [4]$$

$$\Phi_{extractives}(\%)=(C-C)_{before\ extraction} - (C-C)_{after\ extraction} \qquad [5]$$

in which a is a correction term for surface contamination and b is a factor used for calculation of lignin from the C-C signal. The value of a depends on the material and the instrument used. In this work, a value of 2% was used for a, an estimate based on hundreds of similar experiments at HUT. Factor b is 2 for a model MWL (Freudenberg and Neish 1968). The apparent surface coverage of polysaccharides was calculated based on the assumption that the surface is totally covered by lignin, extractives and polysaccharides and was obtained as the difference (100 - coverage of lignin - coverage of extractives)%.

The O/C atomic ratios, calculated from the wide scans, were compared with the percentages of C-C carbon in high-resolution C 1s spectra to estimate the quality of the measurements. Average values for the surface coverage of lignin, extractives and polysaccharides as well as standard deviations for these values were calculated from the three replicate analyses.

5.2.3 AFM

AFM measurements were made using a Nanoscope IIIa Multimode instrument from Digital Instruments Inc. at the Laboratory of Forest Products Chemistry, HUT, Espoo,

Finland. AFM topography and phase images were obtained in the tapping mode using Pointprobe tips (NCH, Nanosensors) with a resonance frequency of 260 – 310 kHz. Measurements were performed in air at room temperature using the moderate tapping force (a set-point ratio between 0.4 and 0.7). No image processing except flattening was carried out. At least five images were taken from each sample.

5.2.4 Field Emission Scanning Electron Microscopy (FE-SEM)

The morphology of pulp fibers and fines was characterized using a field emission scanning electron microscope (FE-SEM, Jeol JSM 6335F) at Top Analytica Oy Ltd., Turku, Finland. A very low acceleration voltage (1 kV) was used. Fibers from the Bauer McNett +14 fraction were prepared for FE-SEM analysis by performing a gradual solvent exchange (water:ethanol) prior to drying in a critical point dryer. This was done to avoid changes in the structure due to surface tension. However, some shrinking of the fibers was seen. Fibers were sputter-coated with a thin layer of Au-Pd.

5.2.5 Image analysis

Different fines fractions were studied with an image analyzer developed by Luukko et al. (Luukko et al. 1997) and further improved by Metso, Finland together with KCL (Krogerus et al. 2002). The image analysis program classifies the fines particles into fibrillar and non-fibrillar material and calculates the mass proportion of fibrillar material. The program also identifies particles having rectangular shape, which is typical of ray cells, and computes their mass proportion.

6 RESULTS AND DISCUSSION

6.1 Peeled pulp

The relative intensities of different lignin structures on the surface of fines (created by the TMP process and isolated from TMP prior to peeling), fiber surface layers (peeled from the fiber surface) and bulk (peeled) fibers were calculated from the ToF-SIMS spectra. The peaks representing methoxyl groups (at 31 m/z) and guaiacyl lignin units (at 137 and 151 m/z) were integrated and normalized to the peak at 77 m/z, which represents the general aromatic units assumed to mostly originate from lignin or lignin-like compounds. In addition, the intensity of the peak at 77 m/z was normalized to the intensity of the peak at 127 m/z, which was used as a marker for polysaccharides (hexosaccharides).

The results showed that the content of aromatic (lignin) units was highest for the fines and the fiber surface material, the lignin contents of which were similar (Fig. 11). The bulk fibers showed a lower content of aromatic units, indicating that there was more lignin on the surface of fines and fiber surface layers than on the bulk fibers. In addition, the structure of lignin was quite similar in fines and fiber surface layers, but differed from that on the bulk fiber surfaces, since there were fewer methoxyl groups and guaiacyl units in the lignin present on the surface of fines and fiber surface layers than on the surface of bulk fibers.
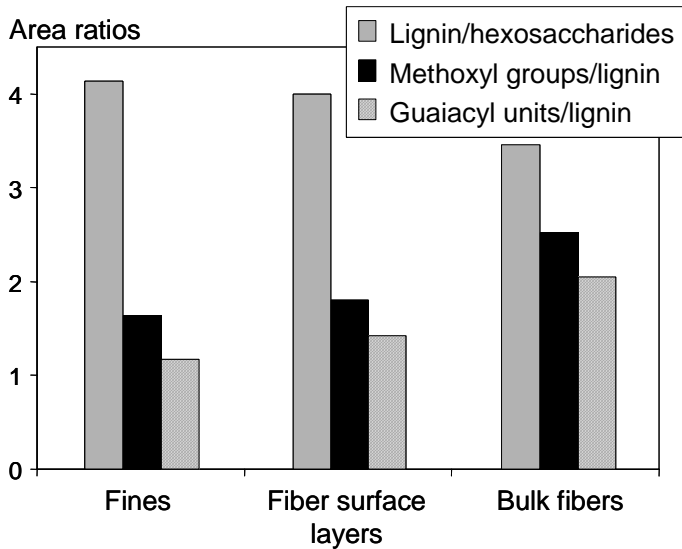
Figure 11. Contents of aromatic units (lignin) and methoxyl and guaiacyl units in lignin on the surface of TMP fines, fiber surface layers and bulk (peeled) fibers.

The peaks originating from sterols/steryl esters and glycerides and from resin acids, saturated fatty acids and unsaturated fatty acids were calculated from positive and negative ToF-SIMS spectra, respectively, and normalized to the total intensity of the spectra (Fig. 12). The results showed that more neutral and acidic extractives covered the surface of the fines and fiber surface layer than of the peeled fibers.

The ToF-SIMS results for different fractions, i.e. fines, fiber surface layers and bulk fibers, are compared in Figs. 11 and 12. However, quantification of ToF-SIMS results and their comparison between different fractions should be performed with care, since the peak intensity in the ToF-SIMS spectrum is known to depend on the matrix, and the spectra of materials with different surface structures (e.g. roughness) are not necessarily directly comparable.
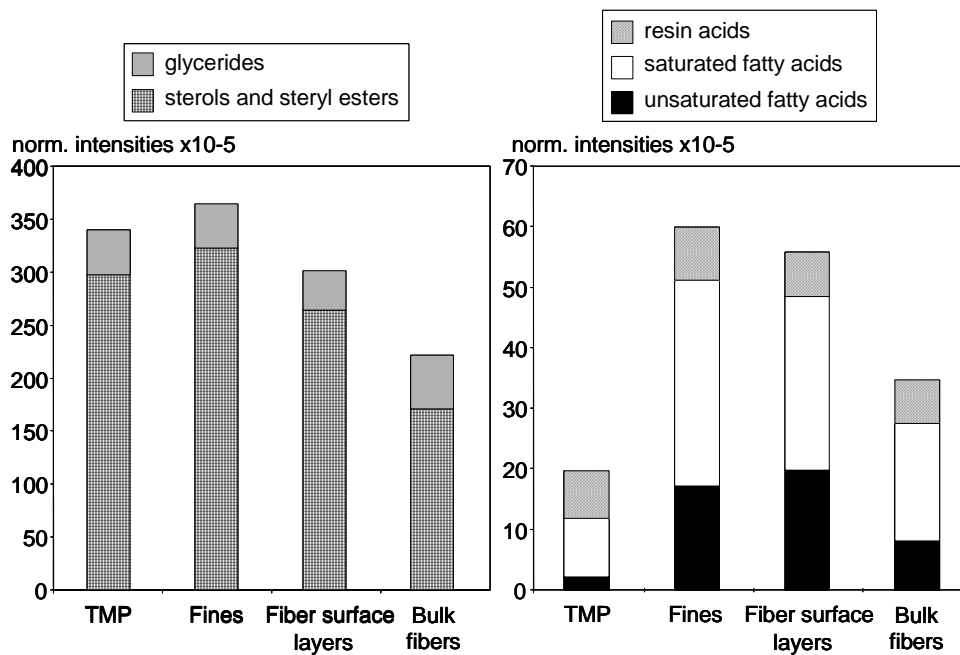
Figure 12. Normalized intensities of different extractives groups on the surfaces of TMP, fines, fiber surface layers and bulk fibers. The peak intensities were normalized to the total intensity of the spectra.

The ESCA/XPS results (Fig. 13) agreed well with the results given by ToF-SIMS. Fines had the highest surface coverage of extractives (20%), followed by fiber surface material (15%), which according to a light microscopy study consisted mainly of fibrils. Interestingly, these fiber surface layer fibrils had a high surface coverage of lignin similar to that of the fines, which was mainly flake-like particles from the middle lamella. Thus fines and fiber surface layers were mostly covered by extractives and lignin, while half of the peeled fiber surfaces (bulk fibers) were covered with polysaccharides and half with lignin and extractives.
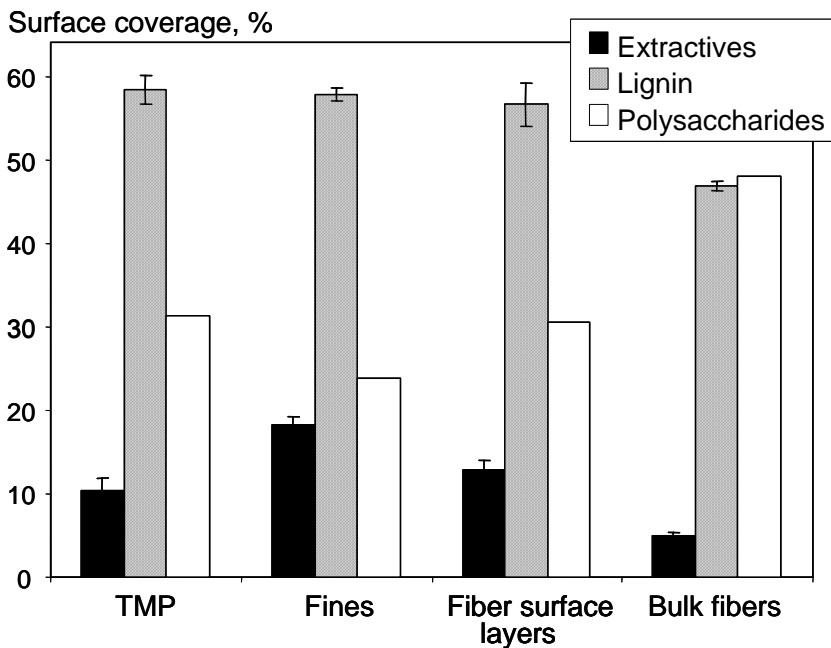
Figure 13. Surface coverage of extractives, lignin and polysaccharides on TMP, fines, fiber surface layers and bulk fibers.

The lateral distribution of surface compounds was studied using imaging ToF-SIMS. In Fig. 14 the positive total ion image of the bulk fiber surface is shown on the left, along with image showing the distribution of lignin (methoxyl groups and aromatic and guaiacyl units) in the middle, and that of extractives (glycerides, sterols/steryl esters and fatty and resin acids) on the right. Both lignin and extractives seem to be evenly distributed on, but not fully covering, the surface of bulk fibers.
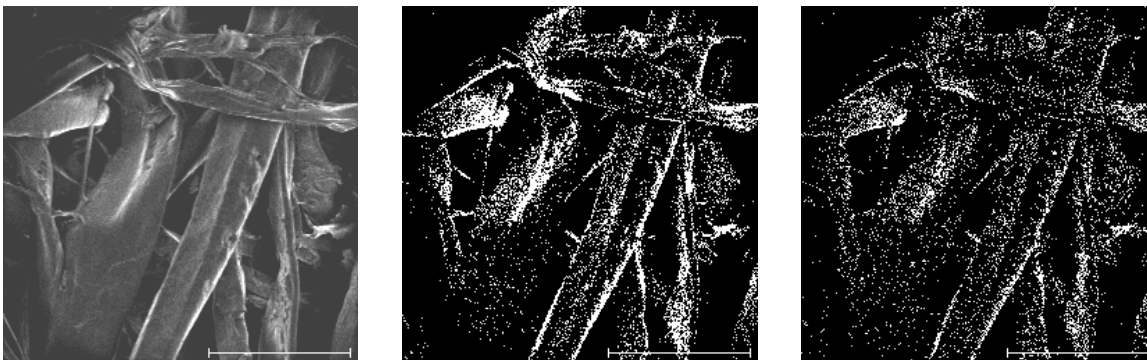

Figure 14. Positive total ion image (left) and the distribution of lignin (middle) and extractives (right) on the surface of bulk fibers. Bar: 100 µm.

6.2 Unbleached pulps

It was found in Papers I and II, that the surface chemical compositions of fibers and different types of fines differ from each other. As already mentioned above, quantitative comparison of different fractions is not straightforward with ToF-SIMS, since the sample matrix may be different in these fractions. Therefore, in the following chapters, pulps are only compared with other pulps, fibers with other fibers etc. to ensure the best possible quantitative results.

6.2.1 Surface chemical composition of pulps and fibers

The contents (peak intensity normalized to the total intensity) of guaiacyl units (137 and 151 m/z) in lignin were similar for the different mechanical pulps (Fig. 15), but differed for the isolated fibers. The content of guaiacyl lignin units was smaller on the surface of CTMP fibers than on the other fibers, indicating that CTMP fibers had a greater covering of outer fiber wall layers and middle lamella than the other fibers, since the guaiacyl lignin content is lower on the surface of outer fiber wall layers than on the surface of inner fiber wall layers (Paper I). GW fibers had the highest content of guaiacyl lignin units on their surface compared to the other pulp fibers, indicating that GW fibers contained more inner fiber wall lignin on the surface. The intensity of guaiacyl lignin units on pulp fibers correlated quite well with the freeness of the pulps (Table 1): the lower the freeness of the pulp, the higher the guaiacyl lignin content. The intensity of guaiacyl lignin units measured from the fibers could therefore be used to estimate the defibration degree of these pulps.
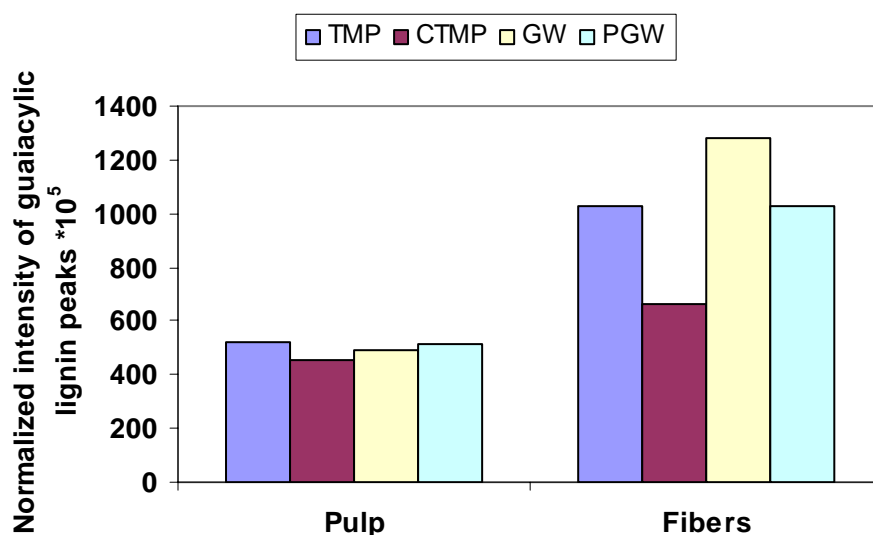

Figure 15. Intensities of positive peaks originating from guaiacyl lignin (137 and 151 m/z) normalized to the total intensity of the spectra on the surface of pulps and fibers by ToF-SIMS.

The ESCA/XPS results showed that the two thermomechanical pulps had very similar surface compositions, as did the groundwood pulps (Fig. 16). The two pulp types differed in their surface chemical composition: thermomechanical pulps had a higher surface area covered by lignin and extractives than the groundwood pulps. The different mechanisms of thermomechanical and groundwood pulp production probably explain the differences in their surface chemical composition. Thermomechanical pulps are produced by refining wood chips, which involves the separation of fibers and development of fibers by a peeling action, which removes material from the fiber surface layer by layer; groundwood pulps, on the other hand, are produced by pressing the logs against a revolving stone, a process that creates shorter fibers and more fines. In the production of CTMP, chemical treatment with sodium sulfite is combined with mechanical defibration, making the lignin in the fiber wall easier to fracture. According to Franzen (Franzen 1986), fiber separation

during CTMP refining takes place in the primary wall, which has a high lignin content, whereas for TMP and PGW fibers, separation occurs mostly in the secondary wall.

The lignin coverage on CTMP fibers was indeed higher than on TMP fibers (Fig. 16, right), because of fiber separation in the highly lignified fiber wall layer. The groundwood pulp fibers were very similar in their surface composition and had a higher surface coverage of polysaccharides and lower surface coverage of lignin than refiner pulps, indicating more fiber separation rupture in the S2 layer.

Together, the ToF-SIMS and ESCA/XPS results showed that the content of guaiacyl lignin units is not a measure of surface coverage of lignin, but a measure of the content of exposed inner wall layers on the surface.
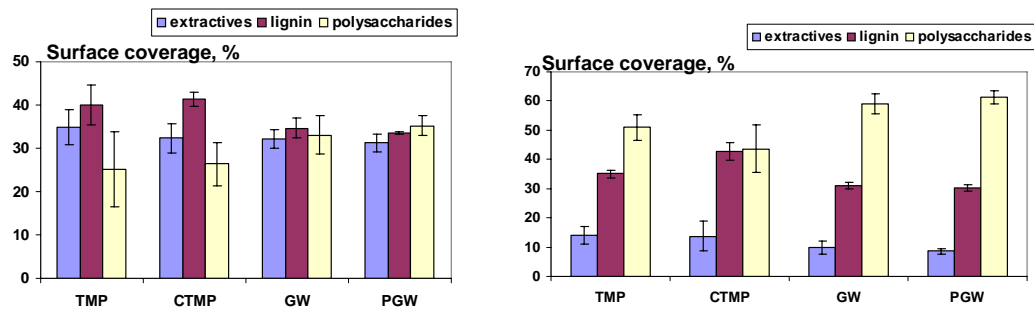

Figure 16. Surface chemical compositions of pulps (left) and fibers (right): TMP, CTMP*, GW* and PGW* determined by ESCA. *Unpublished data.

GW pulp had a slightly higher content of free and esterified fatty acids on its surface as shown by ToF-SIMS (Fig. 17), but the coverage of extractives was similar to that of the other pulps (Fig. 16, left), indicating smaller content of other extractives such as sterols and steryl esters. Fibers isolated from the pulps contained only a fraction of the original fatty acids on their surfaces, and ESCA/XPS also showed a decrease in the coverage of extractives on the fiber surfaces (Fig. 17). Most of the original pitch present in the pulp had probably become dispersed during hot disintegration and fractionation of the pulp and had thus been removed from the fiber surfaces.
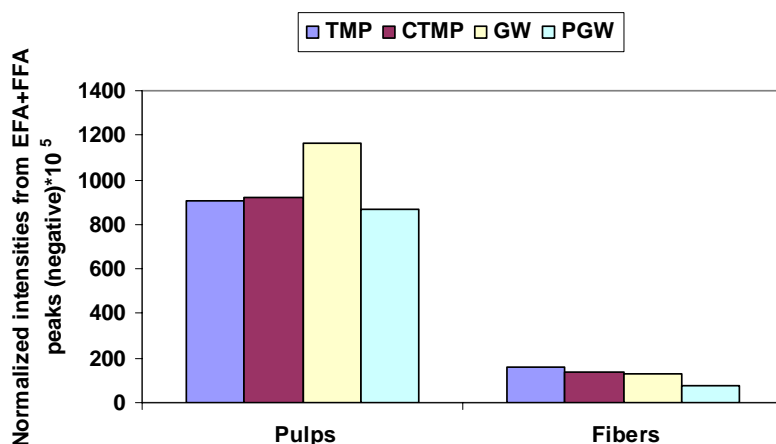
Figure 17. Intensities of negative peaks originating from esterified and free fatty acids (EFA+FFA) normalized to the total intensity of the spectra on the surface of pulps and fibers analyzed by ToF-SIMS.

6.2.2 Surface chemical composition of fines: fibrils and flakes

Fibrils isolated from groundwood pulps had a slightly higher content of guaiacyl lignin units on their surface (Fig. 18) than those from refiner pulps, indicating that they originated more from the inner fiber wall layers. The opposite was true for flakes. Interestingly, fibrils from refiner pulps had lower content of guaiacyl lignin on their surface, as though they originated from outer fiber wall layers than flakes. This result could possibly be explained by the high content of extractives adsorbed on the surface of fibrils, thus masking the presence of guaiacyl lignin units.
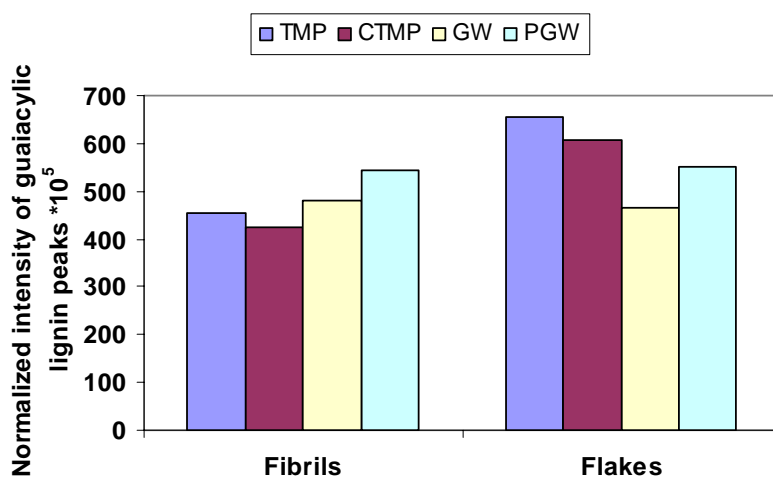
Figure 18. Intensities of positive peaks originating from guaiacyl lignin (137 and 151 m/z) normalized to the total intensity of the spectra on the surface of isolated fibrils and flakes by ToF-SIMS.

Fibrils isolated from refiner pulps had a higher surface coverage of lignin than those isolated from groundwood pulp (Fig. 19, left), indicating that they originated more from the lignin-rich outer fiber wall layers (P+S1) and thus supporting the result given by ToF-SIMS. Flakes from refiner pulps also had a higher coverage of lignin on their surface than

those from groundwood pulps, indicating outer fiber wall origin. However, ToF-SIMS results showed that flakes from refiner pulps had higher contents of guaiacyl lignin units than groundwood pulps, indicating that they originated more from the inner fiber wall layers. The reason for this discrepancy is possibly the presence of lignin-rich ray cells in the flakes fraction of refiner pulps, which increased the surface coverage of lignin.
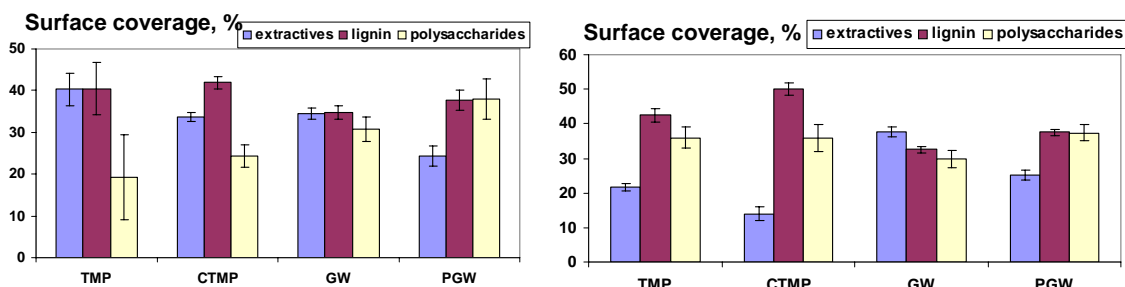
Figure 19. Surface chemical compositions of fibrils (left) and flakes (right): TMP, CTMP*, GW* and PGW* determined by ESCA. *Unpublished data.

The fibrils isolated from the mechanical pulps had surfaces fairly rich in extractives, as shown by both ESCA/XPS (Fig. 19) and ToF-SIMS (Fig. 20). At first, this result seemed surprising and doubtful, since fibrils have been considered to originate from the secondary wall and to have a high content of polysaccharides (Heikkurinen and Hattula 1993). However, fibrils also have a high specific surface area (Wood et al. 1991) and presumably a high cellulose content on their surface (Sundberg et al. 2003). They would therefore be ideal material for the extractives present mainly in colloidal form in the process waters to adsorb/deposit on. The pulps were hot-disintegrated prior to fractionation and all accessible extractives on the surface were probably either dissolved or dispersed into the water. However, it was concluded in Paper II that the water removed from the fibrils by centrifugation contained more extractives than the fibrils, so that less dissolved and colloidal particles were adsorbed/deposited on the fibril surfaces than remained in the water. It was also shown in Paper II that, based on their bulk chemistry, the fibrils studied in this work probably originated from the primary cell wall layer, since their surface chemistry was different from that of fibrils from the secondary wall. These results support the results presented in Paper I.

The difference between refiner and groundwood pulps could also be seen in the free and esterified fatty acids present on the surface of fines (Fig. 20). The intensity of fatty acid peaks on TMP and CTMP fibrils was high, while flakes had only a small intensity of peaks originating from esterified and free fatty acids, as did fibers. Groundwood pulps had a high intensity of fatty acid peaks on the surfaces of both fibrils and flakes, indicating that fibrils and flakes had a similar surface contents of extractives. CTMP fibrils had a lower surface coverage of extractives than TMP fibrils (Fig. 19). PGW fibrils also had lower surface coverage of extractives than GW fibrils. This may be due to different process conditions such as the use of sulfonation and higher temperature and pressure in the CTMP and PGW processes, respectively.

The surface coverage of extractives on flakes isolated from refiner pulps was significantly lower than that on groundwood pulps (Fig. 19), which is in good agreement with the results from ToF-SIMS. The fibrils and flakes in groundwood pulps showed greater

similarities in their surface than the fibrils and flakes in refiner pulps. Again the surface coverage of extractives was higher on TMP flakes and GW flakes than on CTMP flakes and PGW flakes, respectively.
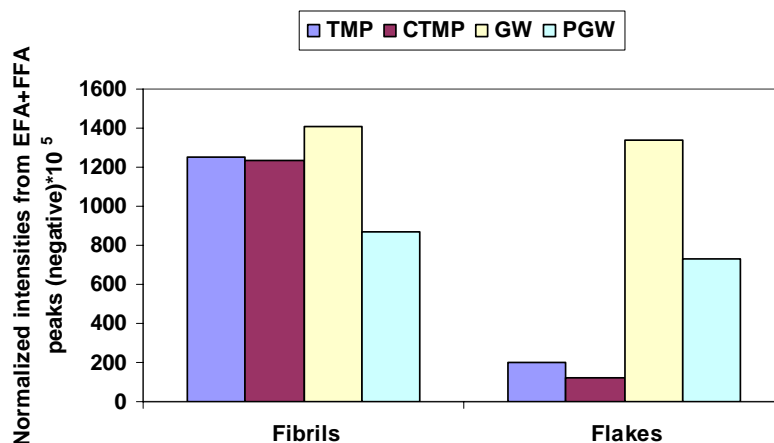

Figure 20. Intensities of negative peaks originating from esterified and free fatty acids (EFA+FFA) normalized to the total intensity of the spectra on the surface of fibrils and flakes measured by ToF-SIMS.

6.2.3 Surface morphological properties of fibers, fibrils and flakes

The surface morphology of TMP and CTMP fibers, fibrils and flakes was studied by AFM. AFM images of fibers separated from TMP showed two types of microfibrillar orientation (Fig. 10, Paper II). In one of the images (Fig. 10a) the orientation of fibrils is random, indicating that the image was from the primary wall (P). In the other image (Fig. 10b) the orientation of fibrils was almost the same as the orientation of the fiber axis, suggesting that the S2 layer had been revealed.

All the AFM phase images obtained for the fibers separated from CTMP looked very much alike. On the left in Fig. 21 the image size is 3x3 μm^2, and the image shows that the whole surface is covered with granular material, which has been interpreted as being lignin (Koljonen 2004). This interpretation was supported by the ESCA/XPS results (Fig. 16), which showed a high surface coverage of lignin on CTMP fibers. On the right in Fig. 21 is a magnification of the same spot on the surface (image size 1.5x1.5 μm^2), showing the shape and distribution of these granules more clearly. The granules appear to be spherical or ellipsoidal in shape and they seem to cover the whole surface of the fiber.
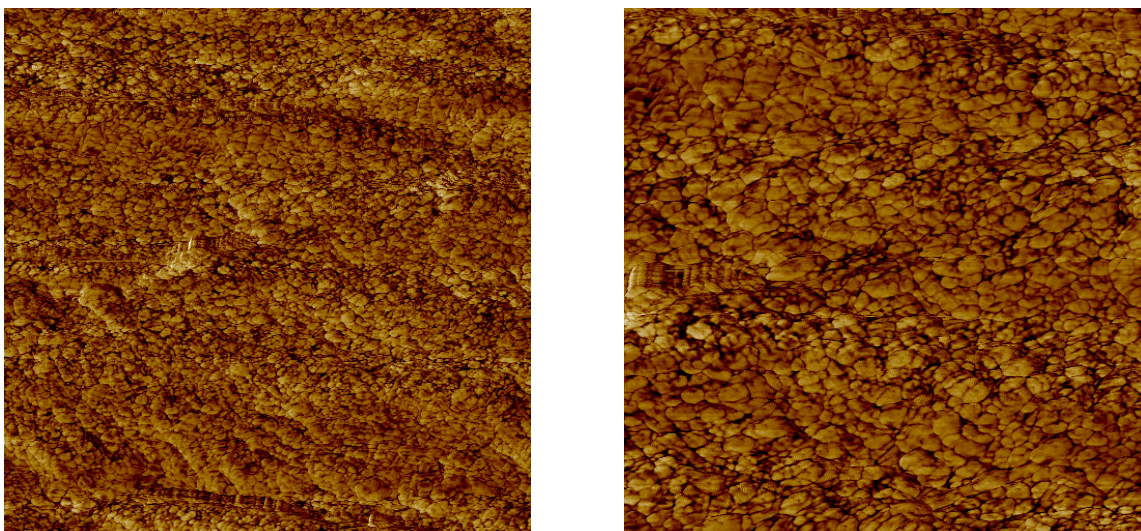
Figure 21. AFM phase images of fibers separated from CTMP. Image size 3x3 µm^2 (left) and 1.5x1.5 µm^2 (right).

AFM phase images of fibrils separated from TMP and CTMP are shown in Fig. 22. Two types of material were seen on the surface of TMP fibrils (Fig. 22, left). The fibrils were shown to be rich in surface extractives and lignin by ToF-SIMS and ESCA/XPS, and it is therefore suggested that the materials seen in the image were extractives and lignin. When light tapping is used in AFM, as in this case, the adhesion between the tip and the sample dominates the phase contrast. Darker areas in the phase contrast image are probably areas with higher water content. The darker, patch-like areas were therefore interpreted as being either lignin or polysaccharides. The dark material also contained small granules, indicating that this material was most probably lignin. The lighter areas covering most of the surface could then be extractives. This conclusion was supported by previously published results (Tammelin 2006). The surface of CTMP fibrils seemed to consist of only one material (Fig. 22, right). Several images were again taken from TMP and CTMP fibrils and all led to the same conclusions.
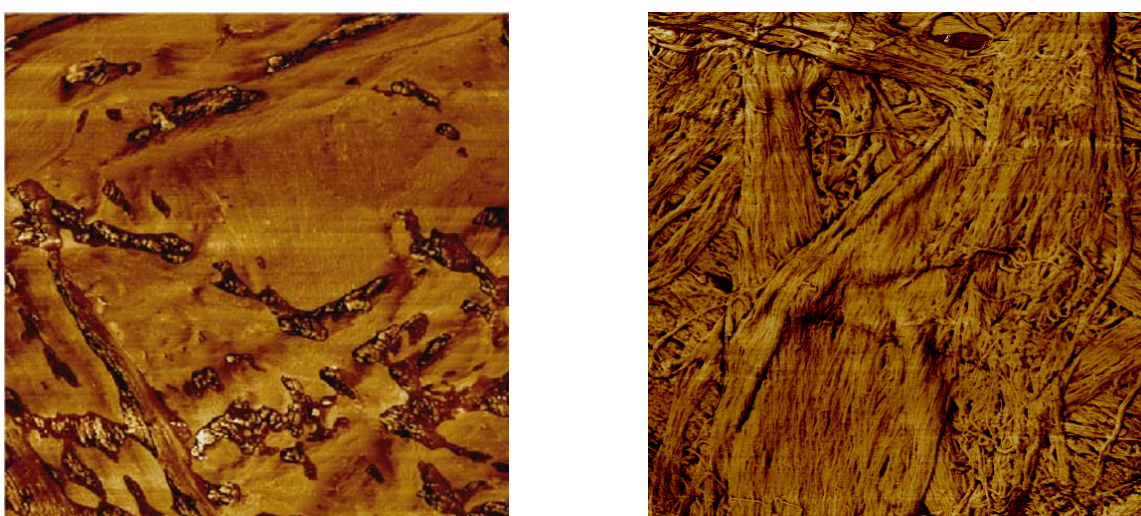

Figure 22. AFM phase images of fibrils isolated from TMP (left) and from CTMP (right). Image size 3x3 µm^2.

Figure 23 shows small (1.5x1.5 µm^2) AFM phase images of flakes isolated from TMP (Fig. 23, left) and CTMP (Fig. 23, right). Granular lignin could be seen on both surfaces. Some

fibrillar orientation could also be seen on the surface of TMP flakes, but not on CTMP flakes. Lighter areas on CTMP flakes could be a film of extractives on granules of lignin.
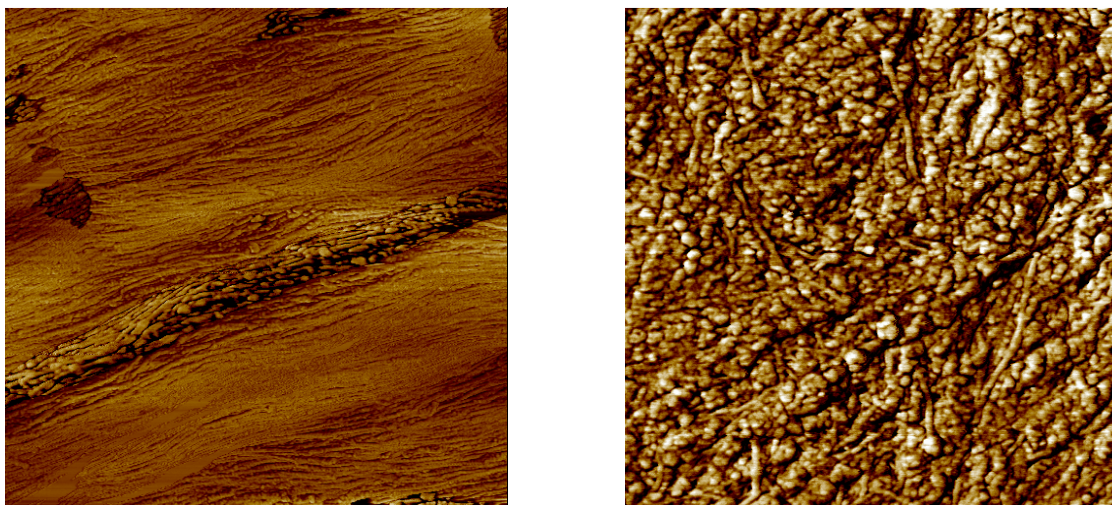
Figure 23. AFM phase images of flakes isolated from TMP (left) and from CTMP (right). Image size 1.5x1.5 μm^2.

6.3 Refined pulps

6.3.1 Surface chemical composition of fibers

The intensities of guaiacyl lignin units at 137 and 151 m/z on the fiber surfaces, normalized to the total intensity of the spectra, were monitored throughout the refining (Fig. 24). A statistically significant difference was found in the content of guaiacyl lignin units between mainline refined (A) and reject-refined pulps (B). The intensity of both lignin peaks increased in the first reject refining stage (B1), indicating that more native S2 fiber wall lignin had been revealed. However, the content of guaiacyl lignin units did not increase further during reject refining or correlate with the freeness of the pulp, as in the case of unbleached pulps (Chapter 4.2.1).

Figure 24. Intensities of peaks from guaiacyl lignin units (G), normalized to the total intensity of the spectra, on the surface of fibers. The intensities were calculated from the positive ToF-SIMS spectra. A1= after the first mainline refinin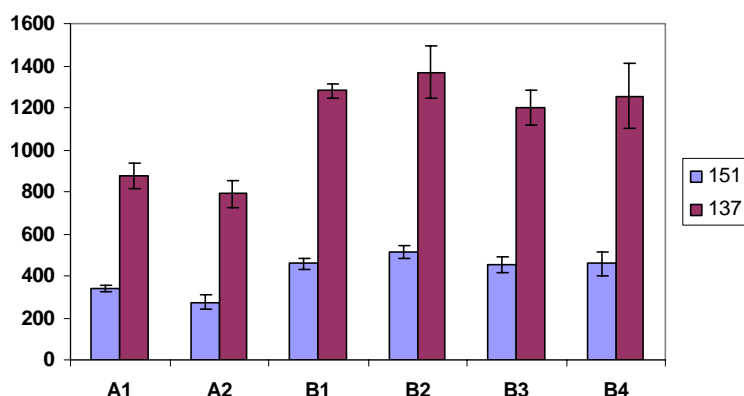g stage (specific energy consumption, SEC 1.55 MWh/t), A2= after the second mainline refining stage (SEC 2.44 MWh/t), B1= after the first reject refining stage (SEC 3.94 MWh/t), B2, B3 and B4= after the two-stage reject refining (SECs 4.44 ,4.65 and 4.88 MWh/t, respectively). Unpublished data.

ESCA/XPS results showed that the surface coverage of lignin was slightly higher on the fibers separated from the mainline refined pulps than on those from the reject refined pulps (Fig. 7, Paper III), indicating that most of the lignin-rich outer surface layers had been removed by the end of the first reject refining stage, some of it probably as fines in the accept. Thus the results from ESCA/XPS and ToF-SIMS together again support the theory that the outer fiber wall layer lignin contains less guaiacyl units than the inner fiber wall layers.

The surface coverage of extractives on fibers isolated from pulps taken after the 1st stage of reject refining showed a decrease (Fig. 7, Paper III), probably as a result of their removal during the screening stage. Dilution of the pulp combined with an increase in temperature probably led to dispersion and dissolution of some of the surface resin. The decrease in the surface coverage of extractives and lignin on the fibers from reject refined pulps led to an increase in the surface coverage of polysaccharides.

With ToF-SIMS, the intensities of esterified and free fatty acids and sterols/steryl esters were found to be smaller on the surface of fibers from reject-refined pulps than on those from mainline refined pulps (Fig. 25), thus supporting the results given by ESCA/XPS.
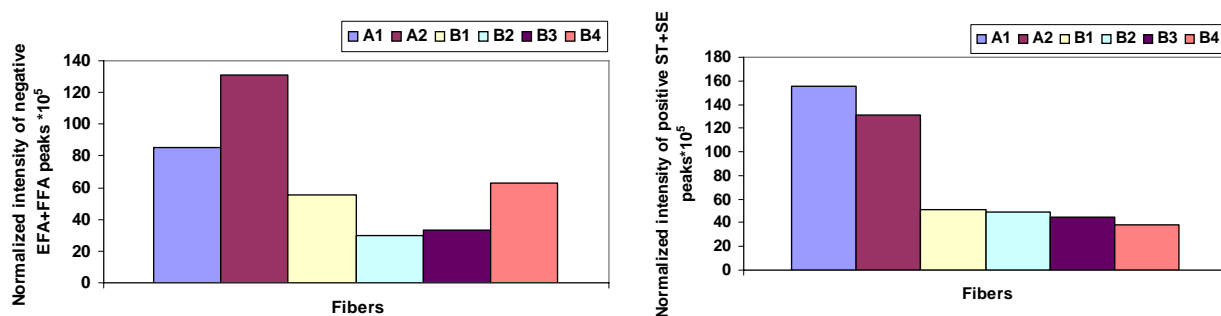
Figure 25. Intensities of peaks from esterified and free fatty acids (left) and from sterols and steryl esters (right) normalized to the total intensity of the spectra on the surfaces of fibers. The intensities of fatty acids were calculated from the negative ToF-SIMS spectra and those of sterols/steryl esters from the positive spectra. A1= after the first mainline refining stage (SEC 1.55 MWh/t), A2= after the second mainline refining stage (SEC 2.44 MWh/t), B1= after the first reject refining stage (SEC 3.94 MWh/t), B2, B3 and B4= after two-stage reject refining (SECs 4.44, 4.65 and 4.88 MWh/t, respectively).

6.3.2 Surface chemical composition of fines: fibrils and flakes

The ToF-SIMS results showed that fibrils had already lost a significant amount of free and esterified fatty acids in the second mainline refining stage, prior to screening, and that screening followed by the first reject refining stage seemingly had no additional influence (Fig. 26, left). The second reject refining stages again removed esterified and free fatty acids from the fibril surfaces. The decrease in the content of fatty acids indicated removal of triglycerides. Sterols and steryl esters were removed sequentially from the surface of fibrils in the refining process (Fig. 26, right). Most of the fatty acids on the surface of flakes had been removed in the first reject refining stage, if not earlier i.e. during screening. About half of the sterols/steryl esters still persisted on the surface of flakes after refining.
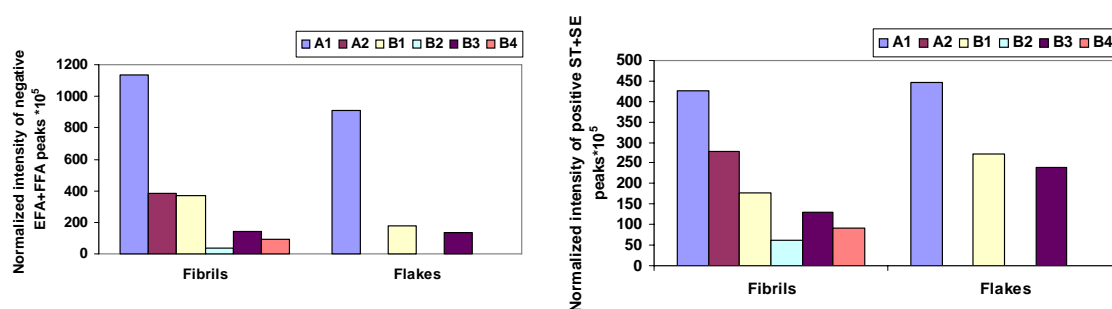
Figure 26. Intensities of peaks from esterified and free fatty acids (left) and from sterols and steryl esters (right) normalized to the total intensity of the spectra on the surfaces of fibrils and flakes. The intensities of fatty acids were calculated from the negative ToF-SIMS spectra and those of sterols/steryl esters from the positive spectra. A1= after the first mainline refining stage (SEC 1.55 MWh/t), A2= after the second mainline refining stage (SEC 2.44 MWh/t), B1= after the first reject refining stage (SEC 3.94 MWh/t), B2, B3 and B4= after two-stage reject refining (SECs 4.44, 4.65 and 4.88 MWh/t, respectively).

The ESCA/XPS results showed that fibrils isolated from the pulps seemed to have lost most of their surface extractives after the two mainline refining stages, prior to screening

(Fig. 27), as also shown by ToF-SIMS. The surface coverage of lignin determined by ESCA/XPS was higher on fibrils isolated from the mainline refined pulps than on those isolated from the reject refined pulps. This indicated that during mainline refining, fibrils were formed to a greater extent from the lignin-rich outer cell wall layers and during reject refining more from the polysaccharide-rich inner cell wall layers. The removal of extractives from the fibril surface may also be partly responsible for the increased polysaccharides coverage.
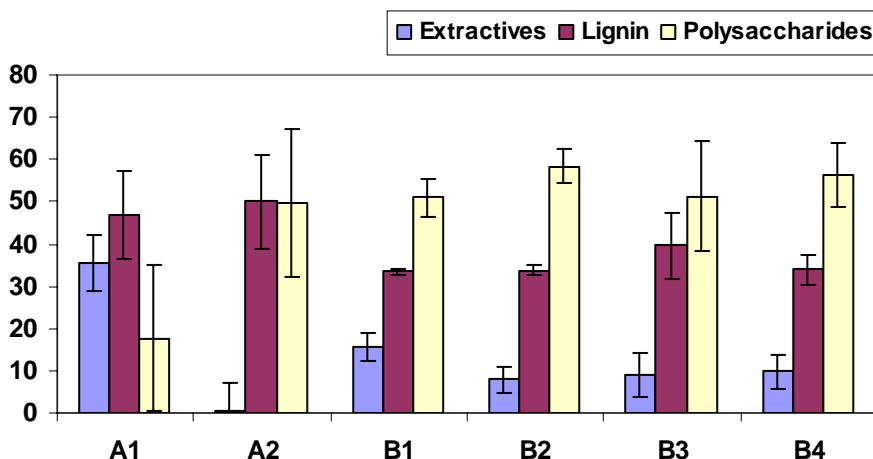

Figure 27. Surface chemical composition of fibrils isolated from the pilot-refined TMP pulps measured by ESCA/XPS. A1= after the first mainline refining stage (SEC 1.55 MWh/t), A2= after the second mainline refining stage (SEC 2.44 MWh/t), B1= after the first reject refining stage (SEC 3.94 MWh/t), B2, B3 and B4= after two-stage reject refining (SECs 4.44, 4.65 and 4.88 MWh/t, respectively). Partly unpublished data.

The surface composition of flakes as measured by ESCA/XPS changed as a function of refining energy (Fig. 8, Paper III). After the first mainline refining stage flakes had a high content of surface extractives and lignin. After the first reject refining stage half of the surface extractives had been removed, probably during screening. The surface coverage of lignin had decreased and that of polysaccharides increased. During the second reject refining stage further changes took place and the surface of flakes was now mostly covered with polysaccharides. These changes were similar to those obtained with fibrils, and indicated that flakes were first formed from the outer fiber wall layers, and that as refining proceeded they were formed from the inner fiber wall layers as well.

Previous publications have stated that lignin-rich flake-like fines and ray cells are formed mainly during the first refining stages, while fibrils containing cellulose are formed during peeling of the cellulose-rich inner fiber wall layers (Heikkurinen and Hattula 1993, Mosbye et al. 2002). It has also been thought that fines originating from middle lamella and primary wall are flake-like particles and that fibrils originate from secondary wall (Mohlin 1997). However, the results from this study showed that both types of fines – fibrils and flakes – were formed throughout the refining process and that their surface chemical composition depended on their origin in the fiber wall. Fines rich in lignin were formed during the early stages of refining and those with more polysaccharide on their surfaces during reject refining. After the second reject refining stage, fibrils and flakes had similar surface chemical compositions.

6.3.3 Surface morphological properties of fibers, fibrils and flakes

FE-SEM was used to obtain images of isolated fibers, fibrils and flakes after the different refining stages. An image of the TMP fiber fraction (Bauer McNett +14) after the first mainline refining stage (Fig. 28, left) showed the mechanism by which outer wall layers were peeled off the fiber surface. Because of the high fibril angle, it is often seen that outer wall layers come off in strips; the remaining outer wall layers were seen as bands surrounding the inner wall layers. This same mechanism has been shown in images published earlier (Moss and Heikkurinen 2003). From the surface chemistry point of view, the outer fiber wall layer was more lignin-rich than the inner wall layer, and as the outer fiber wall layers were peeled off, the surface lignin content decreased.

An image taken of fibers separated from the pulp after the second reject refining stage showed part of a fiber whose surface still retains some of the outer wall layers (Fig. 28, right). However, it could be seen that the outer wall layer was no longer tightly bonded to the inner wall layer and that the fiber wall had started to delaminate. Also, it could be seen how fibrillar lamellae were formed at the boundary between the two layers. Such lamellae may contribute to the amount of flake-like fines in the pulp.

Figure 28. FE-SEM images of a fiber fraction isolated from TMP after the first mainline refining stage (A1, SEC 1.55 MWh/t), left, and after the second reject refining stage (B3, SEC 4.65 MWh/t), right. Magnification 2 000x. Paper III.

The FE-SEM images taken from the fibrils at 10 000x magnification showed that the fibrils isolated from the pulp taken after the first mainline refining stage were generally wider (Fig. 29, left) than the fibrils separated from the pulp after the second reject refining stage (Fig. 29, right). The latter had been broken into smaller fibrils and seemed to form a tight network or lamellae of fibrils. 10-15 images at different magnifications were taken from each fraction, so the images shown below could be considered as representative.
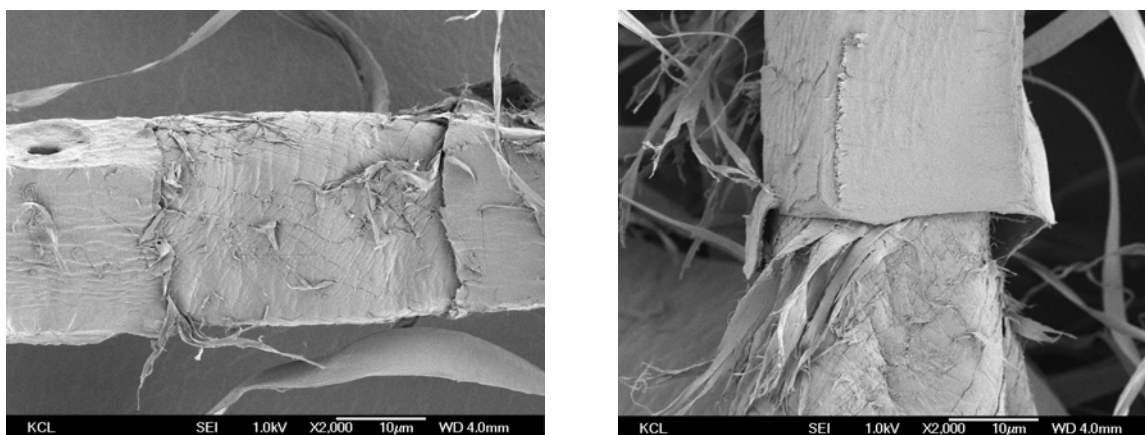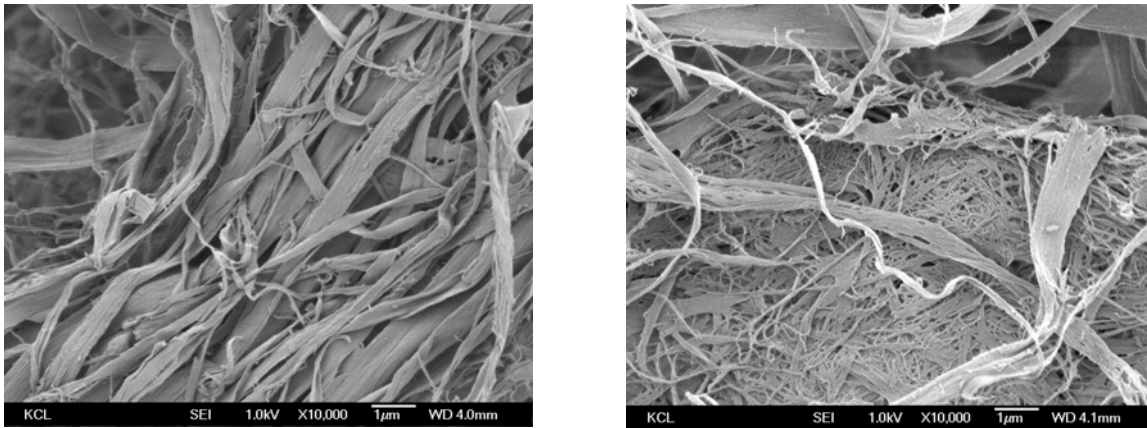
Figure 29. FE-SEM images of a fibril fraction isolated from TMP after the first mainline refining stage (A1, SEC 1.55 MWh/t), left, and after the second reject refining stage (B3, SEC 4.65 MWh/t), right. Magnification 10 000x. Unpublished images.

A comparison of FE-SEM images of flakes isolated from the pulps after the first mainline refining stage and after the second reject refining stage showed that flakes after the first mainline refining stage contained more fibrils attached to them than those from the second reject refining stage (Fig. 30). This was probably due to the fact that the S1 wall layer pulled out the first fibril lamella from S2 as the fiber surface delaminated. The attached fibrils were then probably pulled off from the flakes in the next refining stage and removed with the accept during screening. From eight to ten images at different magnifications were taken from each fraction, so the images shown here could be considered as representative.
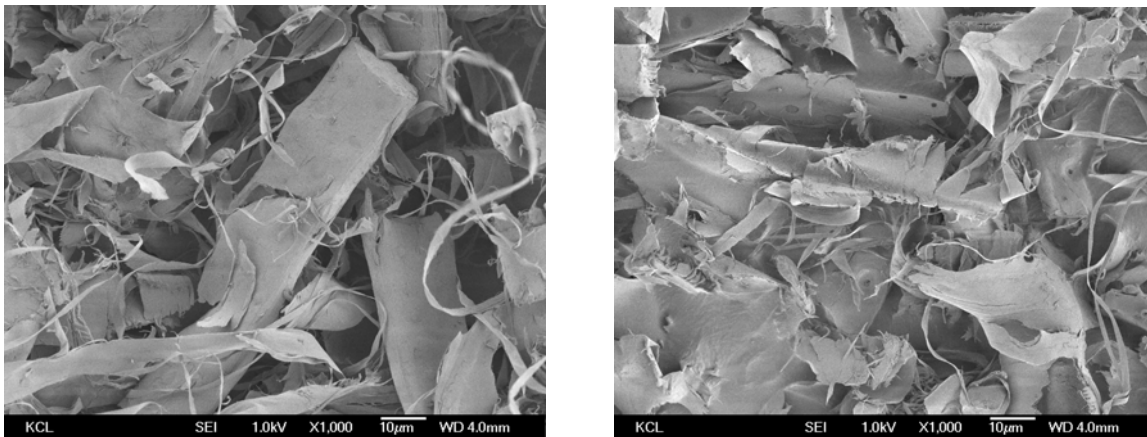
Figure 30. FE-SEM images of flakes isolated from TMP after the first mainline refining stage (A1, SEC 1.55 MWh/t), left, and after the second reject refining stage (B3, SEC 4.65 MWh/t), right. Unpublished images.

6.4 Bleached pulps

6.4.1 Surface chemical composition of pulps and fibers

ToF-SIMS analysis showed that bleaching of TMP and CTMP had no effect on the surface content of guaiacyl lignin units and methoxyl groups; however, chromophores (here represented by coniferaldehydes) were removed by peroxide bleaching (Fig. 31), as expected based on the literature (Svensson Rundlöf et al. 2006). On the surface of fibers,

the content of guaiacyl lignin units and methoxyl groups increased during the peroxide bleaching of TMP and, to a lesser extent, of CTMP. Dithionite bleaching of TMP also resulted in a higher content of guaiacyl units in lignin and of methoxyl groups. In Papers I, II and III, the increased content of guaiacyl units has been taken as an indication of an increased amount of inner fiber wall lignin. According to the literature (Dence 1996), the methoxyl content should decrease during peroxide bleaching in the bulk of pulp. However, in the present work the increase in methoxyl content correlated well with the increase in guaiacyl lignin peak intensity on the fiber surfaces. The increase of guaiacyl lignin and methoxyl groups could be interpreted to mean that peroxide bleaching uncovered more native fiber lignin on the outermost surfaces of fibers, probably due to removal of surface extractives. It may be noted that this did not exclude the possibility that peroxide bleaching had also oxidized part of the surface lignin.
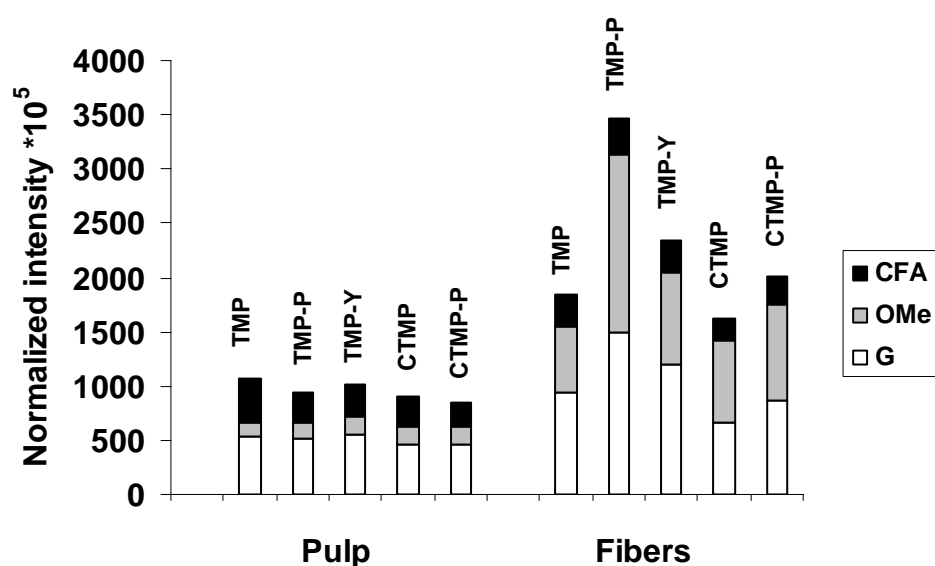

Figure 31. Normalized intensities of peaks originating from lignin structures calculated from positive ToF-SIMS spectra on the surfaces of unbleached and bleached pulps and fibers. P = peroxide bleached, Y=dithionite bleached. G=guaiacyl lignin, OMe=methoxyl group and CFA=coniferaldehyde (representing lignin chromophores) .

The changes in the content of extractives on the pulp surface that resulted from the bleaching of TMP were small as determined by ToF-SIMS (Fig. 32). The content of resin acids decreased slightly, indicating the reaction of hydrogen peroxide with conjugated double bonds in peroxide bleaching (Holmbom 2000). Dithionite bleaching had no notable effect on the surface extractives, as expected (Holmbom 2000). ESCA/XPS results were well in accordance (Fig. 2A, Paper IV) with ToF-SIMS results, showing only a small decrease in the surface coverage of extractives. For CTMP, the changes in the surface extractives content were larger: ToF-SIMS analysis showed some removal of fatty acids, while ESCA/XPS showed a decrease of about 50% in the surface coverage of extractives. Taken together, these results suggest that the extractives composition on the outermost layers remained more or less the same, but that the extractives layer became thinner.

In the case of TMP fibers the most pronounced change was seen for sterols/steryl esters with a smaller change for free and esterified fatty acids, all of which were removed from

fibers during peroxide bleaching (Fig. 32), probably due to high alkalinity. A decrease in the surface coverage of extractives during peroxide bleaching was also shown by ESCA/XPS (Fig. 2B, Paper IV). The content of fatty acids on fibers decreased during the peroxide bleaching of CTMP, indicating removal of triglycerides. This result correlated well with the ESCA/XPS analysis, which showed a decrease in the surface coverage of extractives to about half of their original coverage.
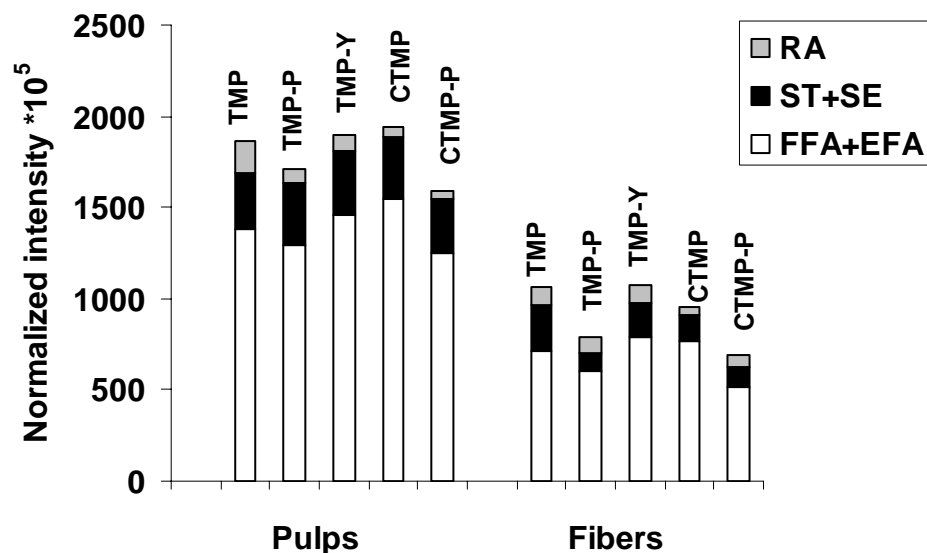

Figure 32. Normalized intensities of peaks originating from extractives on unbleached and bleached pulps and fibers. P = peroxide bleached, Y = dithionite bleached. FFA+EFA = free and esterified fatty acids, ST+SE = sterols/steryl esters and RA = resin acids. Peak intensities were normalized to the total intensity of the spectra.

6.4.2 Surface chemical composition of fines: fibrils and flakes

The intensity of the guaiacyl lignin peak was the same before and after peroxide bleaching on TMP and CTMP fibrils, as well as on fibrils isolated from dithionite-bleached TMP, according to ToF-SIMS (Fig. 33). The intensity of chromophore peaks on fibrils decreased slightly during the peroxide bleaching of TMP.

The intensities of guaiacyl lignin peaks on TMP flakes increased during peroxide bleaching (Fig. 33). The increase in the content of guaiacyl units in lignin was also observed for fibers (Fig. 31), and both results were presumably obtained because peroxide bleaching uncovered more native fiber lignin on the outermost surfaces. The intensity of peaks from methoxyl groups on TMP flakes increased during dithionite bleaching (Fig. 33), as did the intensity of the guaiacyl lignin peak, albeit to a lesser extent. The opposite was observed for CTMP flakes during peroxide bleaching, which resulted in decreased contents of both guaiacyl lignin units and methoxyl groups, possibly due to deposition of extractives onto the surface of flakes, as shown by ToF-SIMS (Fig. 34).
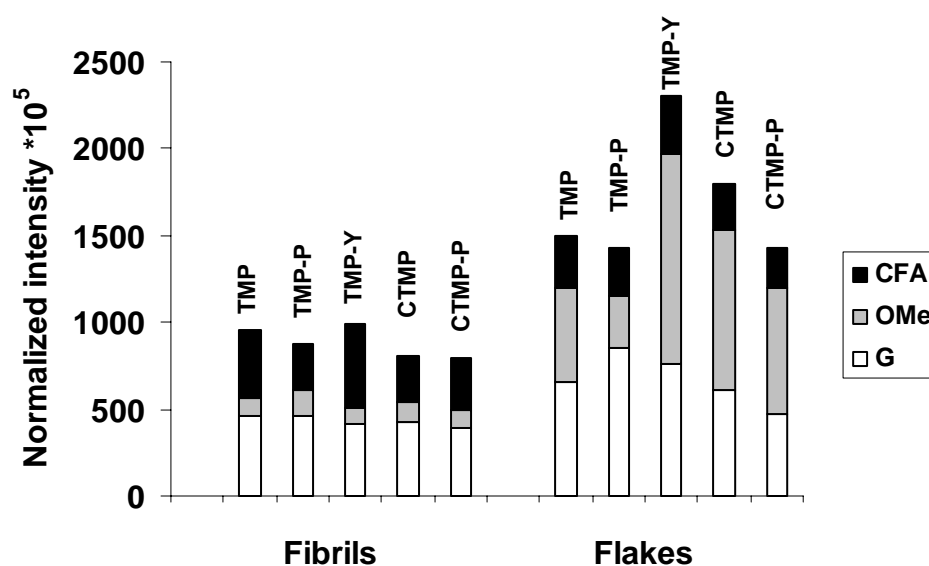
Figure 33. Normalized intensities of peaks originating from lignin structures on unbleached and bleached fibrils and flakes. P = peroxide bleached, Y = dithionite bleached. G = guaiacyl lignin, OMe = methoxyl group and CPH = chromophores. Peak intensities were normalized to the total intensity of the spectra.

The content of resin acids on the surface of TMP fibrils decreased more than that of the other extractives studied during peroxide bleaching (Fig. 34). Slight decreases were also seen for free and esterified fatty acids and sterols/steryl esters on fibrils from TMP-P. The opposite was observed for fibrils from dithionite-bleached TMP and peroxide-bleached CTMP, in which the content of free fatty acids and sterols/steryl esters actually increased. These results were supported by the results from ESCA/XPS (Fig. 2C, Paper IV). The reason for the increased surface content of extractives ion CTMP could the loss in steric stability of colloidal pitch and its adsorption to the surface of CTMP fibrils (Sundberg et al. 1996). In the case of dithionite-bleached TMP, the low pH might have had an influence.

The surface extractives on flakes were less affected by the bleaching operations. There was a slight increase in the content of fatty acids on the surface of flakes due to bleaching and a decrease in the content of sterols/steryl esters on flakes during the peroxide bleaching of TMP. The ESCA/XPS results indicated a larger decrease in the surface coverage of extractives on flakes during both peroxide and dithionite bleaching (Fig. 2D, Paper IV). The contradictory results given by ToF-SIMS and ESCA could be explained by the difference in the analysis depth of these two methods. ToF-SIMS only produces information from the very surface of the sample, while ESCA/XPS analyses a thicker layer of the sample surface. When a film of extractives on the surface becomes thinner, this can be detected with ESCA but not with ToF-SIMS.

The removal of extractives from pulps during dithionite bleaching is not supported by literature (Holmbom 2000) and it may be noted that sample preparation may have influenced the results somewhat.
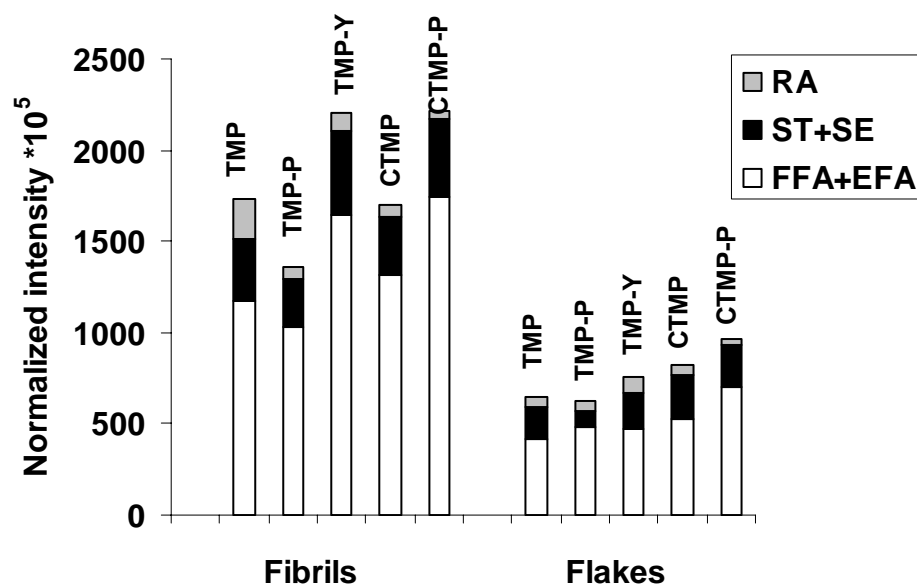
Figure 34. Normalized intensities of peaks originating from extractives on unbleached and bleached fibrils and flakes. P = peroxide bleached, Y = dithionite bleached. FFA+EFA = free and esterified fatty acids, ST+SE = sterols/steryl esters and RA = resin acids. Peak intensities were normalized to the total intensity of the spectra.

The combined results from ToF-SIMS and ESCA showed different types of fines to have different bleaching responses. On the surface of fibrils, it was the extractives that were mainly affected, while on flakes it was the structures in the lignin. Flakes are generally considered harder to bleach than fibrils (Haugan and Gregersen 2006), which may be due to the high specific surface area of fibrils, providing area for surface reactions. Similar results were obtained in this work.

6.5 Enzymatically treated pulps

6.5.1 Surface chemical composition of pulps and fibers

The ToF-SIMS results showed that the content of guaiacyl units in lignin decreased on the surfaces of both pulps and fibers during laccase treatment (Fig. 35, left), probably due to oxidation of the phenolic units in lignin (Kirk and Shimada 1985) and/or redeposition of oxidized and polymerized lignans (Buchert et al. 1999). The intensity of peaks originating from polysaccharides on pulp surfaces increased during the xylanase and lipase treatments, possibly due to removal of xylan and extractives from the surfaces (Fig. 35, right). However, the surface coverage of polysaccharides as determined by ESCA/XPS showed no change within the limits of experimental error (Fig. 36), indicating that these changes were very small and took place on the outermost surface of pulps and therefore could only be detected by the more sensitive ToF-SIMS.

On the surface of fibers, the intensity of guaiacyl lignin peaks increased during xylanase, mannanase and lipase treatments, probably due to removal of xylan, glucomannan and extractives, respectively, thus exposing native lignin (Fig. 35, left). However, the removal of glucomannan and xylan could not be verified with ToF-SIMS, since the intensity of peaks originating from polysaccharides was increased by mannanase treatment and was

unchanged by xylanase treatment. The reason was probably the exposure of cellulose (Fig. 35, right). According to ESCA/XPS analysis, the surface coverage of lignin was increased by xylanase and mannanase treatments, while the surface coverage of polysaccharides was increased by the lipase treatments, partly supporting the results given by ToF-SIMS (Fig. 1A, Paper V).

Figure 35. Intensities of guaiacyl lignin units (G, left) and peaks originating from polysaccharides (PS, right) on pulps* and fibers. The peak values were obtained from the positive ToF-SIMS spectra and normalized to the total intensity of the spectra (Paper V, *unpublished results).
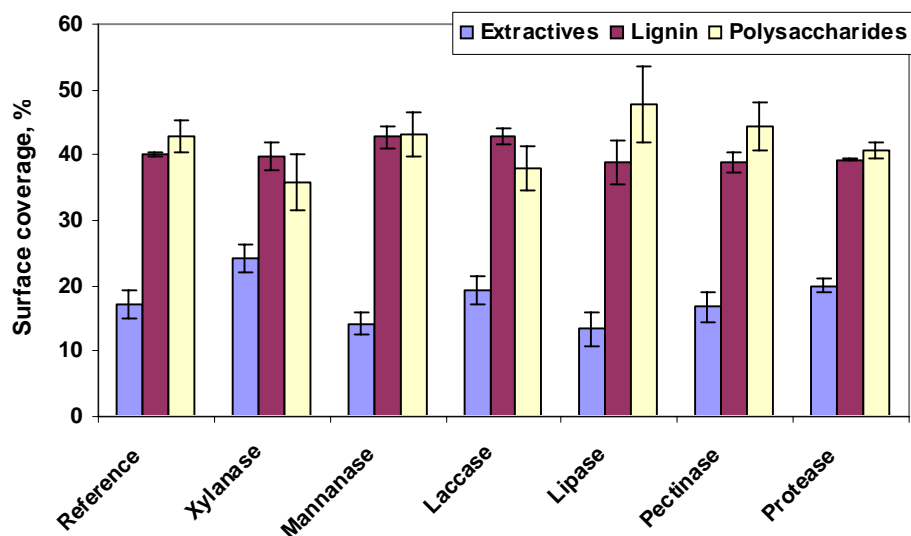
Figure 36. Surface chemical compositions (% area) of enzymatically treated pulps determined by ESCA. Unpublished results.

According to ToF-SIMS analysis, xylanase, mannanase, lipase and laccase treatments had the biggest influence on the composition of surface extractives on pulps and fibers (Fig. 37). Triglycerides were effectively removed by the lipase and laccase treatments, due to hydrolysis of triglycerides into free fatty acids and glycerol and possibly also to oxidation of fatty acids in the triglycerides (Fig. 37, left). Xylanase increased the content of triglycerides on both pulps and fibers, while the effect of mannanase was limited to fibers (Fig. 37, left). The reason behind this could be destabilization of colloidal pitch and

its adsorption onto the fiber surface, which is known to occur during mannanase and xylanase treatments (Kantelinen et al. 1995).

Laccase treatment was found to lower the content of resin acids on the surfaces of both pulp and fibers (Fig. 37, right). Laccase has been reported to attack fatty acids with several double bonds and resin acids containing conjugated structures (Karlsson, Holmbom et al. 2001). Mannanase treatment also seemed to destabilize resin acids, causing them to deposit on the surface of pulp, but not on fibers. Xylanase treatment did not have this effect.

Pectinase and protease treatments had only a small effect on the surface chemical composition of pulps and fibers. In Paper V, it was also concluded that these treatments were not very effective towards pectin and proteins, respectively.
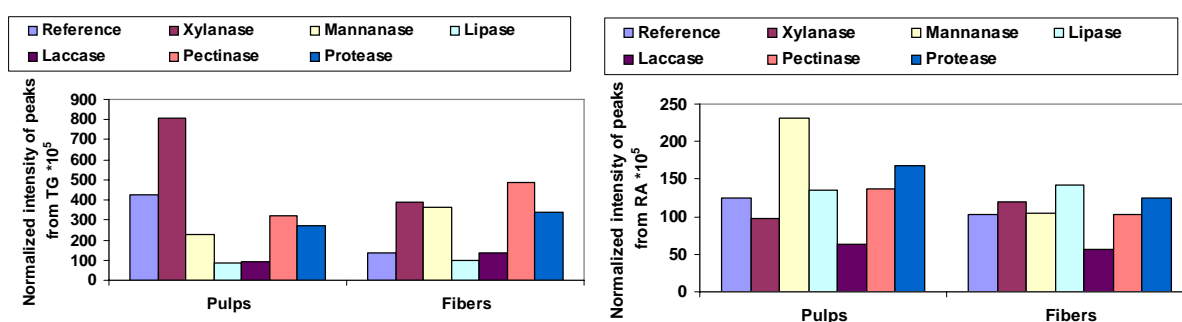
Figure 37. Intensities of peaks originating from triglycerides (TG) and resin acids (RA) on the surface of pulps and fibers. The peaks were calculated from the positive ToF-SIMS spectra and normalized to the total intensity of the spectrum (Paper V).

6.5.2 Surface chemical composition of fines: fibrils and flakes

Laccase treatment also reduced the amount of guaiacyl lignin units on the surfaces of fibrils and flakes (Fig. 38, left), probably due to oxidation of the phenolic units in the surface lignin and/or redeposition of oxidized and polymerized lignans as already discussed above. The intensity of peaks originating from polysaccharides increased during lipase treatment on the surfaces of both fibrils and flakes, probably due to removal of triglycerides, thus exposing polysaccharides underneath. However, no increase in the surface coverage of polysaccharides on fibrils and flakes was observed with ESCA/XPS (Figs. 1B and 1C, Paper V), indicating that the changes took place on the outermost surface of the fibrils and flakes and were thus detected only by ToF-SIMS analysis.
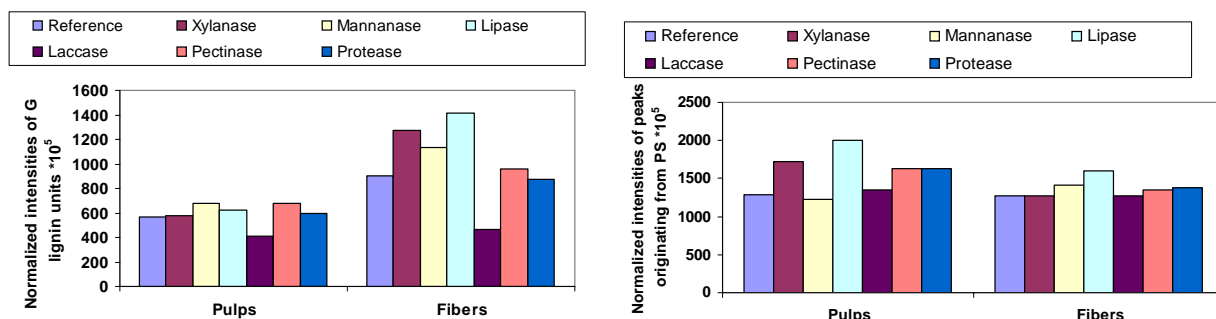
Figure 38. Intensities of guaiacyl lignin units (G, left) and peaks originating from polysaccharides (PS, right) on fibrils and flakes. The peak values were obtained from the positive ToF-SIMS spectra and normalized to the total intensity of the spectra (Paper V).

Triglycerides were selectively removed from the fibrils by lipase and laccase treatments (Fig. 39, left) as from fiber surfaces. Protease treatment also managed to remove triglycerides from the surface of flakes, while pectinase treatment increased their content. The effect of protease was possibly due to removal of triglycerides with other surface components, and that of pectinase to destabilization and redeposition. The content of sterols/steryl esters on fibril and flake surfaces also decreased due to laccase treatment. On the surface of flakes, mannanase and laccase treatments caused a slight decrease in sterol/steryl ester content, while lipase treatment resulted in an increase. According to the ESCA/XPS analysis, the surface coverage of extractives decreased during all the enzymatic treatments (Fig. 1B, Paper V) on fibrils. Selective removal of extractives from the surface of fibrils was obtained with lipase and laccase and the effect of other treatments was probably the removal of triglycerides, together with other surface components, from fibrils. The changes in the surface composition of flakes as analyzed by ESCA/XPS were small and within the limits of experimental error (Fig. 1C, Paper V), indicating that they took place on the outermost surface.
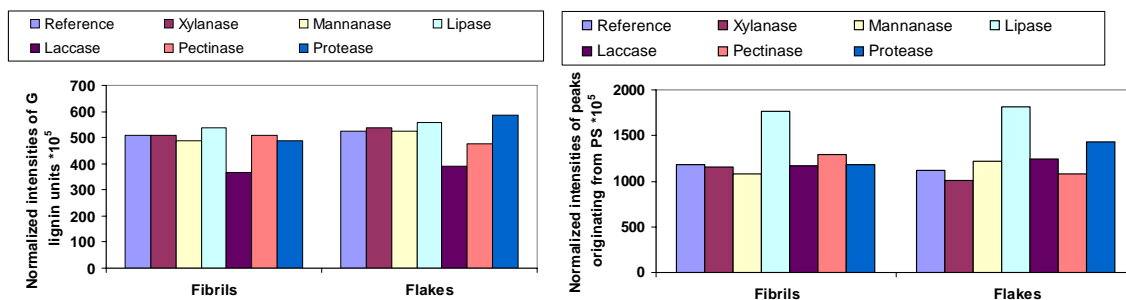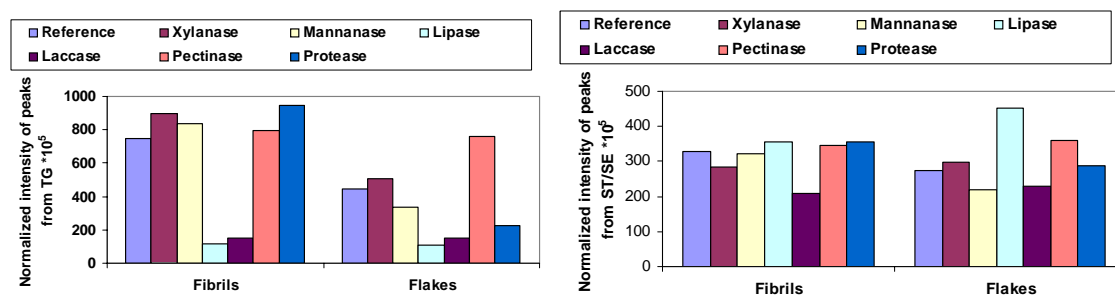

Figure 39. Intensities of peaks originating from triglycerides (TG) and sterols/steryl esters (ST/SE) on the surface of pulps. The peaks were calculated from the positive ToF-SIMS spectra and normalized to the total intensity of the spectrum (Paper V).

7 CONCLUSIONS

ToF-SIMS proved to be a valuable tool for studying the surface chemical properties of mechanical pulps, fibers and fines as well as the effects of increased specific energy consumption, bleaching and enzymatic treatments on these properties. The most interesting results were obtained by analyzing the intensity of peaks originating from guaiacyl units in lignin and from different extractives. The ToF-SIMS results were generally supported by the results given by ESCA/XPS, although some discrepancies were found, possibly due to differences in analysis depth and/or sensitivity. Unlike ESCA/XPS, ToF-SIMS cannot be considered to be a quantitative analysis method for organics. However, ToF-SIMS does not suffer from analytical inaccuracy caused by inadequate extraction of samples.

Surface morphological studies conducted using AFM gave some additional information about the physical appearance of surface lignin, extractives and polysaccharides. The distribution of these surface components could also be studied. FE-SEM gave valuable information about the changes in the surface morphology resulting from increases in refining energy consumption.

The first part of this work, in which the TMP fiber surface was peeled off mechanically, showed that different layers of the wood fiber differ in their surface chemical properties and that it is worth studying the surfaces of different particles in mechanical pulps. The surfaces of fines created in the mainline refining process were rich in lignin, because they have been created from the outer layers of the fiber wall. Fines surfaces also contained large amounts of extractives, since they had a high surface area and colloidal extractives are readily adsorbed or deposited onto them. The content of guaiacyl units in lignin increased when inner fiber wall layers were exposed.

The analysis of different mechanical pulps revealed that their surface chemical properties differed due to differences in defibration mechanisms and process conditions (e.g. chemical treatments and increased pressure), thus supporting the fracture mechanism hypothesis presented by Franzen (1986). It was possible to isolate fibers and two different types of fines, fibrils and flakes, from the pulps. The surface chemical and morphological properties of these pulp fractions varied according to the pulp and to the fraction in question. Groundwood fibers had a more polysaccharide-rich surface than the fibers from refiner pulps. Fibrils and flakes from groundwood pulps differed less in their surface chemistry than fibrils and flakes from refiner pulps. CTMP fibers not only had higher surface lignin coverage than TMP fibers, but the morphology of the surface lignin was also very different. Fibers were generally the fraction with the highest surface coverage of polysaccharides, while fibrils were rich in extractives adsorbed/deposited onto their surface, and flakes contained both lignin and extractives on their surface.

The refining experiments showed that the surface properties of fibers, fibrils and flakes changed constantly as refining proceeded. Outer layers of fiber wall were removed, although some remnants still persisted on the fiber surface after quite harsh refining. Fibrils and flakes were both formed throughout the refining process, first from the outer fiber wall layers in mainline refining and slowly increasing in their content of inner wall

layers and polysaccharide coverage during reject refining. The content of adsorbed/deposited pitch was managed by screening. The content of guaiacyl units in lignin was higher on fibers from reject refining than from mainline refining, indicating that inner fiber wall layers were exposed to a greater extent in reject-refined fibers. The chemical analysis results obtained by ToF-SIMS were confirmed by electron microscopy.

The result of bleaching mechanical pulps depended not only on the bleaching chemical and the pulp type, but also on the pulp fraction. Fibers and flakes generally responded to the bleaching chemicals in a similar way. The biggest changes during bleaching were seen on the surface of fibrils, and these changes were due to removal or adsorption/deposition of extractives onto their surfaces. In the case of fibers, the guaiacyl units in lignin were increased by both peroxide and dithionite bleaching. With ToF-SIMS, it was also possible to follow the fate of lignin chromophores on the surface of mechanical pulps during bleaching.

Enzymatic treatments were shown to modify the surface chemical properties of pulps and also to act differently on different pulp fractions. Lipase and laccase removed triglycerides from the surface of pulps and pulp fractions. Laccase also attacked other extractives on the surface. However, lignans were oxidized and deposited on the surface during laccase treatment. Lipase treatment increased the content of polysaccharides in all pulp fractions. Lipase and laccase treatment combined with washing could be used to selectively remove extractives from the pulp surfaces.

Although the experiments performed in this work were done with only one wood species, Norway spruce, the results could be used to predict the surface properties of mechanical pulps, fibers and fines made of other wood species. However, one has to keep in mind the differences between the wood species when making such predictions, such as the differences in the content of extractives and different type of wood cells in the species.

Surface properties of mechanical pulps are important for the quality of end products containing mechanical pulps. Surface properties are known to influence the bonding of pulp fibers and thus the strength of the resulting paper or cartonboard. Surface extractives are probably critical in this respect, especially on the surface of fibrils, normally known to enhance the bonding and strength properties. It was shown in this thesis that there is a risk for the surface of fibrils to become covered with extractives, and this should be avoided.

Adsorption and spreading of water, coating color and printing inks onto the paper surface are also partly controlled by the papers' surface properties. Printing of newsprints, magazine papers and packaging boards is better controlled, and the print quality optimized if we are aware of the composition of the surface and its energy level. Surface analytical techniques, such as ToF-SIMS, ESCA/XPS and contact angle analysis could therefore help us in the prediction of the print quality.

REFERENCES

(1993): Determination of Acetone-Soluble Matter. Test Method SCAN-CM 49:93., Scandinavian Pulp, Paper and Board Testing Comm., Stockholm, Sweden.

Aimoto, K., Aoyagi, S., Kato, N., Iida, N., Yamamoto, A. and Kudo, M. (2006): Evaluation of secondary ion yield enhancement from polymer material by using ToF-SIMS equipped with a gold cluster ion source. Appl. Surf. Sci. 252(2006), 6547-6549.

Benninghoven, A. (2001): The history of static SIMS: A personal perspective. Chapter 2 in ToF-SIMS. Surface analysis by mass spectrometry (ed. J. C. Vickerman and D. Briggs), IM Publications and SurfaceSpectra Ltd, Huddersfield, UK, pp 41-72.

Björkman, A. (1956): Studies on finely divided wood. Part I. Extractions of lignin with neutral solvents. Svensk Papperstidning 60 (1956), 477-485.

Braaten, K. R. (1997): The impact of fibre geometry, fibre splitting and fibrillation on light scattering. International Mechanical Pulping Conference, June 9-13, 1997, Stockholm, Sweden, pp 349-353.

Brecht, W. and Klemm, K. (1953): The mixture of structures in a mechanical pulp as a key to the knowledge of its technological properties. Pulp Paper Mag. Can. 54(1953):1, 72-80.

Brinen, J. S. (1993): The observation and distribution of organic additives on paper surface using surface spectroscopic techniques. Nord. Pulp Paper Res. J. 8(1993):1, 123-129.

Brinen, J. S., Greenhouse, S. and Dunlop-Jones, N. (1991): SIMS (secondary ion mass spectrometry) imaging: A new approach for studying paper surfaces. Nord. Pulp Paper Res. J. 6(1991):2, 47-52.

Brinen, J. S. and Kulick, R.J. (1995): SIMS imaging of paper surfaces. Part 4. The detection of desizing agents on hard-to-size paper surfaces. Int. J. Mass Spectrom. Ion Proc. 143 (1995), 177-190.

Brinen, J. S. and Kulick, R. J. (1996): Detection of ASA and desizing agents in hard to size paper surfaces by SIMS. 1996 International Paper and Coating Chemistry Symposium, June 11-13, 1996, Ottawa, Canada, pp 125-129.

Brinen, J. S. and Proverb, R. J. (1991): SIMS imaging of paper surfaces. Part 2. Distribution of organic surfactants. Nord. Pulp Paper Res. J. 6(1991):4, 177-183.

Buchert, J., Mustranta, A., Spetz, P., Ekman, R. and Luukko, K. (1999): Use of enzymes for modification of dissolved and colloidal substances in process waters of mechanical pulping. Pre-Symposium of the 10th ISWPC: Recent advances in Pulp Science and Technology, June 2-4, 1999, Seoul, Korea, pp 115-119.

Börås, L. and Gatenholm, P. (1999a): Surface composition and morphology of CTMP fibers. Holzforschung 53(1999):2 188-194.

Börås, L. and Gatenholm, P. (1999b): Surface properties of mechanical pulps prepared under various sulfonation conditions and preheating time. Holzforschung 53(1999):4, 429-434.

Dalton, J. S., Preston, J. S., Heard, P.J., Allen, G.C., Elton, N.J. and Husband, J.C. (2002): Investigation into the distribution of ink components throughout printed coated paper. Part 2: Utilizing XPS and SIMS. Colloids Surfaces A 205 (2002), 199-213.

de Silveira, G., Forsberg, P. and Conners, T.E. (1995): Scanning Electron Microscopy: A tool for the analysis of wood pulp fibers and paper.Chapter 2 in Surface analysis of paper (ed. T. E. Conners and S. Banerjee), CRC Press Inc., Boca Raton, FL, USA, pp 41-71.

Delcorte, A., Poleunis, C. and Berdrand, P. (2006): Stretching the limits of static SIMS with C_{60}^+. Appl. Surf. Sci. 252 (2006), 6494-6497.

Dence, C. W. (1996): Chemistry of mechanical pulp bleaching. Chapter III 4 in Pulp Bleaching. Principles and Practice (ed. C. W. Dence and D. W. Reeve), TAPPI Press Atlanta, GA, USA, pp 163-181.

Deslandes, Y., Pleizier, G., Poire, E., Sapieha, S., Wertheimer, M.R. and Sacher, E. (1998): The surface modification of pure cellulose paper induced by low-pressure nitrogen plasma treatment. Plasmas Polymers 3(1998):2, 61-76.

Dorris, G. M. and Gray, D. G. (1978): The surface analysis of paper and wood fibres by ESCA. II. Surface composition of mechanical pulps. Cellulose Chem. Technol. 12(1978):6, 721-734.

Fardim, P. and Duran, N. (2002): Surface chemistry of Eucalyptus wood pulp fibres: effects of chemical pulping. Holzforschung 56(2002):6, 615-622.

Fardim, P., Gustafsson, J., von Shoultz, S., Peltonen, J. and Holmbom, B. (2005): Extractives of fiber surfaces investigated by XPS, ToF-SIMS and AFM. Colloids Surfaces A 255(2005), 91-103.

Fardim, P. and Holmbom, B. (2005): Origin and surface distribution of anionic groups in different papermaking fibres. Colloids and Surfaces A 252(2005), 237-242.

Fardim, P. and Holmbom, B. (2005): ToF-SIMS imaging: a valuable chemical microscopy technique for paper and paper coatings. Appl. Surf. Sci. 249(2005), 393-407.

Franzen, R. (1986): General and selective upgrading of mechanical pulps. Nord. Pulp Paper Res. J. 1(1986):3, 4-13.

Freudenberg, K. and Neish, A. C. (1968): Constitution and Biosynthesis of Lignin (ed. H. G. Wittmann), Springer-Verlag, Berlin, Germany, pp 103.

Fukushima, K., Yamauchi, K., Saito, K., Yasuda, S., Takahashi, M. and Yoshi, T. (2001): Analysis of lignin structures by ToF-SIMS. 11th International Symposium on Wood and Pulping Chemistry (ISWPC), June 11-14, 2001, Nice, France, pp 327-329.

Goldstein, J. I., Newbury, D. E., Echlin, P, Joy, D.E., Romig, A.D., Jr., Lyman, C.E., Fiori, C. and Lifshin, E. (1992): Scanning Electron Microscopy and X-ray Microanalysis. A text for biologists, material scientists, and geologists. Plenum Press, New York, USA, pp 34.

Hanley, S. J. and Gray, D. G. (1994): Atomic force microscope images of black spruce wood sections and pulp fibres. Holzforschung 48(1994):1, 29-34.

Hanley, S. J. and Gray, D. G. (1995): Atomic Force Microscopy. Chapter 14 in Surface analysis of paper (ed. T. E. Conners and S. Banerjee), CRC Press, Inc., Boca Raton, FL, USA, pp 301-324.

Hannuksela, T., Fardim, P. and Holmbom, B. (2003): Sorption of spruce O-acetylated galactoglucomannans onto different pulp fibres. Cellulose 10(2003):4, 317-324.

Haugan, M. and Gregersen, O. (2006): Hydrogen peroxide bleaching of TMP fines. J. Pulp Paper Sci. 32(2006):4, 209-216.

Heikkurinen, A. and Hattula, T. (1993): Mechanical pulp fines - Characterization and implications for defibration mechanisms. 18th International Mechanical Pulping Conference, June 15-17, 1993, Oslo, Norway, pp 294-308.

Holmbom, B. (2000): Resin reactions and deresination in bleaching. Chapter 9 in Pitch control, wood resin and deresination (ed. E. L. Back and L. H. Allen), TAPPI Press Atlanta, GA, USA, pp 231-244.

Imai, T., Tanabe, K., Kato, T. and Fukushima, K. (2005): Determination of ferruginol, a heartwood diterpene phenol, in Cryptomeria japonica by time-of-flight secondary ion mass spectrometry (ToF-SIMS). 59th Appita Annual Conference and exhibition, ISWFPC (International Symposium on Wood, Fibre and Pulping Chemistry), May 16-19, 2005, Auckland, New Zealand, paper 27, pp 153-157.

Istone, W. K. (1994): Static secondary ion mass spectrometry and x-ray photoelectron spectroscopy for the characterization of surface defects in paper products. J. Vacuum Sci. Technol. A: Vacuum, Surfaces, and Films 12(1994):4, 2525-2522.

Istone, W. K. (1995): X-Ray photoelectron Spectroscopy (XPS). Chapter 11 in Surface analysis of paper (ed. T. E. Conners and S. Banerjee), CRC Press, Inc., Boca Raton, FL, USA, pp 235-268.

Johnsen, P. O., Skinnarland, I., Helle, T. and Houen, T.J. (1995): Distribution of lignin and other materials on particle surfaces in mechanical pulps. 1995 International Mechanical Pulping Conference, June 12-15, 1995, Ottawa, Canada, pp 93-107.

Kantelinen, A., Jokinen, O., Sarkki, A.-L., Pettersson, C., Sundberg, K., Eckerman, C., Ekman, R. and Holmbom, B. (1995): Effect of enzymes on the stability of colloidal pitch. 8th International Symposium on Wood and Pulping Chemistry (ISWPC), June 6-9, 1995, Helsinki, Finland, pp 605-612.

Karlsson, S., Holmbom, B., Spetz, P., Mustranta, A. and Buchert, J. (2001): Reactivity of Trametes laccases with fatty and resin acids. J. Appl. Microbiol. Biotechnol. 55(2001), 317-320.

Karnis, A. (1994): The mechanisms of fibre development in mechanical pulping. J. Pulp Paper Sci. 20(1994):10, J280-J288.

Kirk, T. K. and Shimada, M. (1985): Lignin biodegradation: the microorganisms involved and the physiology and biochemistry of degradation by white-rot fungi. Chapter in Biosynthesis and biodegradation of wood components (ed. T. Higuchi), Academic Press Inc., Orlando, FL, USA, pp 579.

Kleen, M. (2000a): Surface chemistry of kraft pulp fibers during TCF bleaching studied by ToF-SIMS. 6th European Workshop on Lignocellulosics and Pulping (EWLP), Sept. 3-6, 2000, Bordeaux, France, pp 41-44.

Kleen, M. (2000b): ToF-SIMS as a new analytical tool for studies of pulp fibre surface chemistry. International symposium on cellulose and lignocellulosics chemistry 2000 (ISCLC 2000), Dec. 16-8, 2000, Kunming, China, pp 290-294.

Kleen, M. (2005): Surface lignin and extractives on hardwood RDH kraft pulp chemically characterized by ToF-SIMS. Holzforschung 59(2005), 481-487.

Kleen, M. and Nilvebrandt, N.-O. (2001): Simultaneous characterization of free and esterified fatty acids and fatty acid salts using Time-of-flight Secondary Ion Mass Spectrometry. Post-Symposium Workshop of the 11th ISWPC, June 18-19, 2001, Grenoble, France, pp 51-54.

Koivula, H., Fardim, P. and Toivakka, M. (2006): Characterization of Pigment Particle Surfaces by ToF-SIMS. 2006 TAPPI Advanced Coating Fundamentals Symposium, Feb. 8-10, 2006, Turku, Finland, session 3, 7 p.

Kokkonen, P., Fardim, P. and Holmbom, B. (2004): Surface distribution of extractives on TMP handsheets analyzed by ESCA, ATR-IR, ToF-SIMS and ESEM. Nord. Pulp Paper Res. J. 19(2004):3, 318-324.

Koljonen, K. (2004): Effect of surface properties of fibres on some paper properties of mechanical and chemical pulp. Doctoral thesis, Helsinki University of Technology, Department of Forest Products Technology, Espoo, Finland, 94 p.

Koljonen, K., Stenius, P. and Buchert, J. (1997): The surface chemistry of PGW pulp fiber fractions. International Mechanical Pulping Conference (IMPC), June 9-13, 1997, Stockholm, Sweden, pp 407-411.

Koljonen, K., Österberg, M., Johansson, L.-S. and Stenius, P. (2003): Surface chemistry and morphology of different mechanical pulps determined by ESCA and AFM. Colloids Surfaces A 228(2003):1-3, 143-158.

Koljonen, K., Österberg, M., Kleen, M., Fuhrman, A. and Stenius, P. (2004): Precipitation of lignin and extractives on kraft pulp: effect on surface chemistry, surface morphology and paper strength. Cellulose 11(2004):2, 209-224.

Krogerus, B., Fagerholm, K. and Tiikkaja, E. (2002). Fines from different pulps compared by image analysis. Nord. Pulp Paper Res. J. 17(2002):4, 440-444.

Kulick, R. J. and Brinen, J. S. (1996): Probing paper surfaces with ToF-SIMS - A new tool for problem solving. 1996 Papermakers conference, March 24-27, 1996, Philadelphia, PA, USA, pp 325-334.

Lidbrandt, O. and Mohlin, U.-B. (1980): Changes in fibre structure due to refining as revealed by SEM. International Symposium on Fundamental Concepts of Refining, Sept. 16-18, 1980, Appleton, WI, USA, pp 61-74.

Lipponen, J., Lappalainen, T., Astola, J. and Gröhn, J. (2004): Novel method for quantitative starch penetration analysis through iodine staining and image analysis of cross-sections of uncoated fine paper. Nord. Pulp Paper Res. J. 19(2004):3, 300-308.

Luukko, K., Kemppainen-Kajola, P. and Paulapuro, H. (1997): Characterization of mechanical pulp fines by image analysis. Appita J. 50(1997):5, 387-392.

Luukko, K., Laine, J. and Pere, J. (1999). Chemical characterization of different mechanical pulp fines. Appita J. 52(1999):3, 126-131.

Mancosky, D. G. and Lucia, L. A. (2001): Use of ToF-SIMS for the analysis of surface metals in H2O2-bleached lignocellulosic fibers. Pure Appl. Chem. 73(2001):12, 2047-2058.

Mancosky, D. G., Lucia, L. A., Brogdon, B.N. and Braun, B.M. (2002): Application of nontraditional technologies to improve the efficiency for the hydrogen peroxide bleaching of pulps. 2002 Fall Technical Conference and Trade Fair, Sept. 8-11, 2002, San Diego, CA, USA, session 16, 10 p.

Matsushita, Y., Ookura, A., Imai, T., Fukushima, K. and Kato, T. (2005): Analysis of behavior of rosin glycerine ester in rosin ester emulsion size by visualization using ToF-SIMS. Japan Tappi J. 59(2005):11, 79-87.

Mohlin, U.-B. (1977): Distinguishing character of TMP. Pulp Paper Can. 78(1977):12, 83-88 (T291-296).

Mohlin, U.-B. (1997): Fiber development during mechanical pulp refining. J. Pulp Paper Sci. 23(1997):1, J28-J33.

Mosbye, J., Laine, J. and Moe, S. (2003): The effect of dissolved substances on the adsorption of colloidal extractives to fines in mechanical pulp. Nord. Pulp Paper Res. J. 18(2003):1, 63-68.

Mosbye, J., Moe, S. and Laine, J. (2002): The charge and chemical composition of fines in mechanical pulp. Nord. Pulp Paper Res. J. 17(2002):3, 352-356.

Moss, P. and Groom, L. (2002): Microscopy. Chapter 5 in Handbook of physical testing of paper, Vol. 2. (ed. J. Borch, M. B. Lyne, R. E. Mark, C. C. Habeger and K. Murakami), Marcel Dekker Inc. New York, USA, pp 149-265.

Moss, P. and Heikkurinen, A. (2003): Swelling of mechanical pulp fibre walls studied by CSLM. International Mechanical Pulping Conference, June 4-7, 2003, Quebec, Que, Canada, pp 293-297.

Mustranta, A., Koljonen, K., Pere, J., Tenkanen, M., Stenius, P. and Buchert, J. (2000): Characterization of mechanical pulp fibres with enzymatic, chemical and immunochemical methods. 6th European Worshop on Lignocellulosics and Pulp (EWLP), Sept. 3-6, 2000, Bordeaux, France, pp 15-18.

Ozaki, Y. and Sawatari, A. (1997): Surface characterization of a rosin sizing agent in paper by means of EPMA, ESCA and ToF-SIMS. Nord. Pulp Paper Res. J. 12(1997):4, 260-266.

Ozaki, Y. and Sawatari, A. (2002): The studies on the distribution of rosin sizing agent in the paper sheet. Part 1: changes in some surface parameters from SEM, ToF-SIMS and ESCA by addition of alum." Res. Bull. Print. Bur. Min. Financ. (2002):72 15-29.

Ozaki, Y. and Uchida, M. (2002): The characterization of water-based gravure ink on coated paper- relationship between the distribution of ink and printability. 11th International Printing and Graphic Arts Conference, Oct. 1-3, 2002, Bordeaux, France, pp session 11, 12 p.

Pachuta, S. J. and Staral, J. S. (1994): Nondestructive analysis of colorants on paper by time-of-flight secondary ion mass spectrometry. Anal. Chem. 66(1994):2, 276-284.

Pascoal Neto, C., Silvestre, A. J. D., Evtuguin, D.V, Freire, C.S.R., Pinto, P.C.R., Santiago, A.S., Fardim, P. and Holmbom, B. (2004): Bulk and surface composition of ECF bleached hardwood kraft pulp fibres. Nord. Pulp Paper Res. J. 19(2004):4, 513-520.

Peltonen, J., Gustafsson, J., Ciovica, L., Lehto, J.H. and Tienvieri, T. (2002): Morphological, surface chemical and mechanical changes of chemical and mechanical pulp fibers during pulping: an atomic force microscopy study. International Pulp Bleaching Conference (IPBC), May 21, 2002, Portland, OR, USA, pp 29-30.

Pere, J., Lappalainen, A., Koljonen, K., Tenkanen, M. and Mustranta, A. (2001): Combination of chemical and immunomicroscopical methods for surface characterization

of mechanical pulp fibres. 11th International Symposium on Wood and Pulping Chemistry, June 11-14, 2001, Nice, France, pp 259-262.

Pinto, J. and Nicholas, M. (1997): SIMS studies of ink jet media. IS&T's NIP13: International Conference on Digital Printing Technologies, Nov. 2-7, 1997, Seattle, WA, USA, pp 420-426.

Reich, D. F. (2001): Sample handling. Chapter 5 in ToF-SIMS. Surface analysis by mass spectrometry (ed. J. C. Vickerman and D. Briggs), IM Publications and SurfaceSpectra Ltd, Huddersfield, UK, pp 113-135.

Reme, P. A., Helle, T. and Johnsen, P.O. (1998): Fibre characteristics of some mechanical pulp grades. Nord. Pulp Paper Res. J. 13(1998):4, 263-268.

Rundlöf, M., Htun, M., Höglund, H. and Wågberg, L. (2000): Mechanical pulp fines of poor quality - Characteristics and influence of white water. J. Pulp Paper Sci. 26(2000):9 308-316.

Saastamoinen, S., Likonen, J. Neimo, L., Paulapuro, H. and Stenius, P. (1994): SIMS study of the adsorption of calcium and aluminium ions on unbleached and hydrogen peroxide bleached pressurised groundwood. Pap. Puu 76(1994):1-2, 74-80.

Saito, K., Kato, T., Takamori, H., Kishimoto, T. and Fukushima, K. (2005a): A new analysis of the depolymerized fragments of lignin polymer using ToF-SIMS. Biomacromol. 6(2005), 2688-2696.

Saito, K., Matsushita, Y., Imai, T., Fukushima, K., Kishimoto, T. and Takamori, H. (2005b): Application of ToF-SIMS to wood analysis. 2005 (72nd) pulp and paper research conference, June 23-24, 2005, Tokyo, Japan, pp 96-101.

Sawatari, A., Sawguchi, M. and Ozaki, Y. (1999): Characterization of rosin on the surface of paper by means of chemical modiifcation - ESCA technique. Pre-Symposium of the 10th ISWPC: Recent advances in Pulp Science and Technology, June 2-4, 1999, Seoul, Korea, pp 349-354.

Schueler, B. W. (2001). Time-of-Flight mass analysers. Chapter 3 in ToF-SIMS. Surface analysis by mass spectrometry (ed. J. C. Vickerman and D. Briggs), IM Publications and SurfaceSpectra Ltd., Huddersfield, UK, pp 75-94.

Sodhi, R. N. S., Sun, L., Sain, M., Farnood, R. and Reeve, D.W. (2005): Ink penetration and printing quality on coated papers studied by time-of-flight secondary ion mass spectrometry (ToF-SIMS) in conjuction with principal component analysis (PCA). 91st Annual Meeting Pulp and Paper Technical Association of Canada, Feb 8-10, 2005, Montreal, QC, Canada, pp C13-16.

Sun, L., Sodhi, R. N. S., Sain, M., Farnood, R. and Reeve, D.W. (2004): Analysis of ink/coating penetration on paper surfaces by time-of-flight secondary ion mass spectrometry (ToF-SIMS) in conjuction with principal component analysis. International Printing and Graphic Arts Conference, Oct. 4-6, 2004, Vancouver, BC, Canada, pp 95-101.

Sundberg, A., Pranovich, A. V. and Holmbom, B. (2003). Chemical characterization of various types of mechanical pulp fines. J. Pulp Paper Sci. 29(2003):5, 173-178.

Sundberg, K., Thornton, J., Holmbom, B. and Ekman, R. (1996): Effects of wood polysaccharides on the stability of colloidal wood resin. J. Pulp Paper Sci. 22(1996):7, J226-230.

Svensson Rundlöf, E., Zhang, E., Zhang, L. and Gellerstedt, G. (2006): The behavior of chromophore structures in softwood mechanical pulp on bleaching with alkaline hydrogen peroxide. Nord. Pulp Paper Res. J. 21(2006):3, 359-364.

Tammelin, T. (2006): Surface interactions in TMP process waters. Doctoral thesis, Helsinki University of Technology, Department of Forest Products Technology, Espoo, Finland, 82 p.

Tan, Z. and Reeve, D. W. (1992): Spatial distribution of organochlorine in fully-bleached kraft pulp fibres. Nord. Pulp Paper Res. J. 7(1992):1, 30-36.

Valton, E., Sain, M. and Schmidhauser, J. (2003): Mechanistic study of cationic styrene-maleic imide resins (SMA I): Surface retention and z-direction penetration in paper using XPS and ToF-SIMS. 89th PAPTAC Annual Meeting, Jan. 27-30, Montreal, QC, Canada, session 1C-1, 5 p.

Vander Wielen, L. C. and Ragauskas, A. J. (2003): Dielectric discharge: A concatenated approach to fibre modification. 12th International Symposium on Wood and Pulping Chemistry (ISWPC), June 9-12, 2003, Madison, WI, USA, pp 373-376.

Wasser, R. B. and Brinen, J.S. (1998): Effect of hydrolyzed ASA on sizing in calcium carbonatefilled paper. Tappi J. 81(1998):7, 139-144.

Westermark, U. (1999): The content of lignin on pulp fiber surfaces. 10th International Symposium on Wood and Pulping Chemistry (ISWPC), June 7-10, Yokohama, Japan, pp 40-42.

Vickerman, J. C. (2001): ToF-SIMS - An overview. Chapter 1 in ToF-SIMS. Surface analysis by mass spectrometry (ed.J. C. Vickerman and D. Briggs), IM Publications and SurfaceSpectra Ltd, Huddersfield, UK, pp 1-40.

Wood, J. R., Grondin, M. and Karnis, A. (1991): Characterization of mechanical pulp fines with a small hydrocyclone. Part I: The principle and nature of the separation. J. Pulp Paper Sci. 17(1991):1, J1-J5.

Wucher, A. (2006): Molecular secondary ion formation under cluster bombardment: A fundamental review. Appl. Surf. Sci. 252(2006), 6482-6489.

Zimmerman, P. A., Hercules, D. M. and Loos, W.O. (1995a): Direct quantitation of alkylketene dimers using time-of-flight secondary ion mass spectrometry. Anal. Chem. 67(1995):17, 2901-2905.

Zimmerman, P. A., Hercules, D. M., Rulle, H., Zehnpfenning, J. and Benninghoven, A. (1995b): Direct analysis of coated and contaminated paper using time-of-flight secondary ion mass spectrometry. Tappi J. 78(1995):2, 180-186.